

Is the central Arctic Ocean a sediment starved basin?

Jan Backman^{a,*}, Martin Jakobsson^b, Reidar Løvlie^c, Leonid Polyak^d,
Lawrence A. Febo^d

^a *Department of Geology and Geochemistry, Stockholm University, Stockholm 10691, Sweden*

^b *Center for Coastal and Ocean Mapping/Joint Hydrographic Center, University of New Hampshire, USA*

^c *Institute of Solid Earth Physics, University of Bergen, Norway*

^d *Byrd Polar Research Center, Ohio State University, USA*

Abstract

Numerous short sediment cores have been retrieved from the central Arctic Ocean, many of which have been assigned sedimentation rates on the order of mm/ka implying that the Arctic Basin was starved of sediments during Plio–Pleistocene times. A review of both shorter-term sedimentation rates, through analysis of available sediment core data, and longer-term sedimentation rates, through estimates of total sediment thickness and bedrock age, suggests that cm/ka-scale rates are pervasive in the central Arctic Ocean. This is not surprising considering the physiographic setting of the Arctic Ocean, being a small land-locked basin since its initial opening during Early Cretaceous times. We thus conclude that the central Arctic Ocean has not been a sediment starved basin, either during Plio–Pleistocene times or during pre-Pliocene times. Rigorous chronostratigraphic analysis permits correlation of sediment cores over a distance of ~2600 km, from the northwestern Amerasia Basin to the northwestern Eurasia Basin via the Lomonosov Ridge, using paleomagnetic, biostratigraphic, and cyclostratigraphic data.

© 2004 Elsevier Ltd. All rights reserved.

1. Introduction

The Arctic Ocean is presently undergoing geoscientific investigations of the type that occurred during the late 1940s through the 1960s in the Atlantic, Indian and Pacific oceans. Seismic reflection and refraction data are scarce in the Arctic Ocean and large areas are virtually unsampled with respect to piston or gravity coring. The vast majority of available cores are < 10 m in length and largely lack biostratigraphically useful calcareous and siliceous microfossils. No drill cores exist from the ridges or deep basins in the central Arctic Ocean. Considering the limited geophysical and geological data available, it is not surprising that hypotheses concerning Arctic Ocean sedimentation rates are currently divergent. The major point of disagreement is whether or not strongly subdued rates of sedimentation persisted in the central Arctic Ocean during Plio–Pleistocene times. The discrepancy between the two scenarios is large enough to represent a major obstacle for improving our understanding of the paleoceanographic and paleoclimatic

development in the central Arctic Ocean and its influence on sub-polar seas.

The low sedimentation rate scenario is based on age models suggesting Plio–Pleistocene rates that vary between about 0.04 and 0.4 cm/ka. This scenario is chiefly derived from cores raised from ridges in the Amerasia Basin and implies that the majority of cores presently available extend well into, or encompasses the entire, Plio–Pleistocene (Clark *et al.*, 1980). A central thought in this scenario is that the low sedimentation rate mode developed when sea-ice first formed, in the Pliocene or earlier (Clark, 1971). One of the T-3 Ice Island geophysicists expressed this idea in the following way (Hall, 1979): “From his investigation of the more than 100 [Alpha Ridge] cores which include probably Middle Pliocene (3.5 Myr BP) material, Clark (1971) was led to conclude that the Arctic Ocean has been frozen since at least the Middle Pliocene, and probably even longer. Low rates of sedimentation have accompanied this ice cover.” Here, we refer to this mode of Arctic sedimentation as ‘sediment starved’.

The contrasting high sedimentation rate scenario is based on age models suggesting rates that vary from about one to a few cm/ka, based on cores from ridges and basins in both the Amerasian and Eurasian parts of

*Corresponding author. Tel.: +46-8-164-720; fax: +46-8-674-7861.
E-mail address: backman@geo.su.se (J. Backman).

the central Arctic Ocean (e.g. Jakobsson et al., 2000a; Nowaczyk et al., 2001). This scenario implies that the formation of sea-ice did not markedly decrease the sediment supply and that most short cores rarely extend beyond the Pleistocene. Erosion and winnowing may have created low (mm/ka-scale) sedimentation rates in the Arctic Basin and, vice versa, the influence of turbidite deposits in the deep basins may have created high sedimentation rates (Grantz et al., 1996, 1999; Darby et al., 1997). These issues are however separate from our key question, which is concerned with the general sediment input to the Arctic Basin through time: whether or not the sediment starved mode was a pervasive condition through Late Neogene, Pleistocene and Holocene times.

The purpose of this paper is to review the two contrasting sedimentation rate scenarios: Have two distinctly different modes of deposition governed the Plio–Pleistocene sedimentation in the Arctic, one slow on a mm/ka-scale and the other less so on a cm/ka-scale? Are the underlying age models of the two depositional modes realistic? If this is the case, can we determine where the two modes apply and why? If this is not the case, can we determine which of the two chronological models to reject? Moreover, we discuss the sedimentation rate history of the Arctic in terms of its physiographic setting, and whether or not the sea-ice cover of the Plio–Pleistocene inhibited the supply of sediments to the central Arctic Ocean. Finally, we present a sediment core correlation along a transect from the southwestern part of the Amerasia Basin to the southwestern part of the Eurasia Basin, which provides a crucial link between the sediment stratigraphies of the two major Arctic Ocean basins.

A handful of short cores exists from the central Arctic Ocean containing sediments of Mesozoic and Paleogene ages (Clark, 1974; Bukry, 1984; Grantz et al., 2001). These cores are not discussed further in this paper because they only represent fragments of older sediment sequences lacking accurate age control and because these cores consequently do not provide insights about sedimentation rates. The several hundred remaining short cores may provide information on Plio–Pleistocene paleoenvironmental conditions and sedimentation rates if their age/depth relationships can be determined. In the absence of drill cores through central Arctic sediment sections the longer-term Miocene through Cretaceous sedimentation history must be estimated from seismic reflection and refraction data showing sediment thickness in combination with tectonic models of seafloor ages.

2. Physiographic setting of the Arctic Ocean

The Arctic Ocean is constrained by the broad continental shelves of the Barents, Kara, Laptev, East

Siberian and Chukchi Seas, the White Sea and the narrow continental shelves of the Beaufort Sea, the Arctic continental margins off the Canadian Arctic Archipelago and northern Greenland. It is a small, virtually land-locked ocean, making up a merely 2.6% of the area, and 1.0% of the volume, of the World Ocean (Jakobsson, 2002). The Fram Strait, a deep passage between northeastern Greenland and northwestern Svalbard, is the only real break in the barrier of continental shelves enclosing the Arctic Ocean. Today, shelf areas occupy as much as 52.9% of the Arctic Ocean total area (Jakobsson et al., 2003a), which is in sharp contrast to the rest of the World's oceans where the combined area of continental shelves and slopes range from 9.1% to 17.7% (Menard and Smith, 1966). The second largest physiographic province in the Arctic Ocean comprises ridges, which again is unique compared to the rest of the World's oceans where abyssal plains dominate (Jakobsson et al., 2003a).

The deep central Arctic Ocean basin is commonly divided into two major sub-basins: (1) the Eurasia Basin, bounded by the Lomonosov Ridge and the shallow shelves of the Barents, Kara, and Laptev Seas and northern Greenland, and (2) the Amerasia Basin bounded by the Lomonosov Ridge and the shelves of the East Siberian, Chukchi, and Beaufort Seas and the Canadian Arctic Archipelago. The Eurasia Basin is subdivided by the Gakkel Ridge into the Amundsen and Nansen Basins and the Amerasia Basin is subdivided by the Alpha-Mendelev Ridge complex into the Canada and Makarov Basins.

The shallow shelves receive huge amounts of sediments discharged from some of the largest rivers on Earth. For example, the Yenisey, Lena, and Ob, together with Pechora, Kolyma, and Severnaya Dvina, drain two-thirds of the entire Eurasian arctic landmass into the Arctic Ocean (Peterson et al., 2002). The catchment area of the Yenisey, Lena, and Ob alone ($8060 \times 10^3 \text{ km}^2$, AARI, 1985) is nearly as large as the entire Arctic Ocean ($9541 \times 10^3 \text{ km}^2$, Jakobsson, 2002). Although the input from rivers must have varied through time, the key physiographic setting of the Arctic Ocean, a small basin surrounded by huge land-masses, has remained constant since its initial opening during presumably Early Cretaceous times. The thick sediment sections on abyssal plains and the extensive continental rises are by-and-large a product of this unique physiographic setting of the central Arctic Ocean.

3. Sedimentation rates from piston, gravity, and box core data

3.1. The mm-scale scenario

A total of 580 short (2–5 m) cores were collected from Ice Island T-3 (Fletcher's Ice Island or Ice Station

Bravo) in the Amerasia Basin between 1952 and 1974 (Weber and Roots, 1990). The concept of low, mm/ka-scale rates, Plio–Pleistocene sedimentation rates in the central Arctic Ocean originates from interpretations of paleomagnetic polarity patterns in these T-3 cores, particularly those that were retrieved from the Alpha and Mendeleev ridges (e.g. Steuerwald et al., 1968; Clark, 1970, 1971, 1996; Hunkins et al., 1971; Herman, 1974; Clark et al., 1980, 2000; Witte and Kent, 1988).

Analysis of the Amerasia Basin CESAR (Canadian Expedition to Study the Alpha Ridge) cores also yielded interpretations in favour of low sedimentation rates (Aksu and Mudie, 1985; Aksu et al., 1988; Scott et al., 1989), as did the study of a few cores from the Lomonosov Ridge (Morris et al., 1985; Spielhagen et al., 1997). Low sedimentation rates have also been suggested for cores retrieved from the periphery of the central Arctic (Northwind Ridge: Poore et al., 1993, 1994; Phillips and Grantz, 2001).

In a crucial synthesis paper published in 1980, Clark and others established 13 correlatable lithostratigraphic units, designated A to M, which include silty and arenaceous lutites, and carbonate-rich, pinkish white layers. The content of sand-sized material was considered to be the key sedimentary characteristic that was used to correlate the 13 lithostratigraphic units “over several hundred thousand square kilometers and in several hundred cores.” Paleomagnetic–lithologic correlations were made in a few cores in which units M through I were interpreted to belong to the Brunhes and upper Matuyama chrons (Clark et al., 1980, Figs. 2, 30; Table 2). The average sedimentation rate during the Brunhes Chron was estimated at 0.11 cm/ka, corresponding to 0.13 cm/ka with an updated age estimate (Shackleton et al., 1990) for the Brunhes/Matuyama boundary. The average rate during the Matuyama Chron was estimated to be 0.07 cm/ka, corresponding to 0.10 cm/ka if using Shackleton’s estimate for the duration of the Matuyama Chron.

The lower part of Clark’s lithostratigraphic units, H through A, was correlated to the geomagnetic polarity timescale (GPTS) in core FL 224, retrieved from the Nautilus Basin north of the Chukchi Plateau. The oldest unit (A) in this core was considered to be of Late Miocene age: “The normal polarity magnetic signatures suggest a maximum age of the oldest undisturbed sediment in FL 224 to be 5.62 Myr. This age is the oldest reliable date for in-place sediment in the Arctic Ocean.” (Clark et al., 1980, p. 24). The 5.62 Ma estimate is based on the timescale of LaBrecque et al. (1977) for the onset of Anomaly 3A, corresponding to base Chron C3An.2n in current terminology (Cande and Kent, 1992) and an age estimate of 6.555 Ma (Shackleton et al., 1995). When using Shackleton’s age estimates of reversal boundaries, the sedimentation rate in the critical core FL 224 is 0.05 cm/ka between top Gauss (2.581 Ma) at

100 cm core depth (within unit D) and top Chron C3An.1n (5.875 Ma) at 255 cm core depth (within unit A; Clark et al., 1980, Fig. 29). These combined paleomagnetic–lithostratigraphic data are at the centre of the ongoing discussion about sedimentation rates in the central Arctic Ocean, as many of the workers that employ Clark’s lithostratigraphic units also tend to employ his age model of these units (e.g. Phillips and Grantz, 1997, 2001; Jokat et al., 1999a). Two different correlations (Minicucci and Clark, 1983; Clark, 1996) between lithologic units A–M and chronostratigraphy are presented in Fig. 1.

Previously, Steuerwald et al. (1968, Fig. 1) and Clark (1970, Fig. 1) placed the Brunhes/Matuyama boundary in the critical core FL 224 at ~1 m core depth. Below 1 m depth in FL 224, the polarity pattern was interpreted differently by these authors, showing no agreement in number or relative length of the polarity zones. Clark et al. (1980, Fig. 29, p. 18) introduced a third interpretation that was “refined in the present study. Interpretations in this paper were augmented by the study and interpretation of physical sedimentological data not previously available.” Here, the number, relative lengths and polarity directions, of the polarity zones, were completely reinterpreted; for example, what had been suggested as the Brunhes normal chron by Steuerwald et al. (1968) and Clark (1970), was considered to be the Matuyama reversed chron by Clark et al. (1980).

The paleomagnetic age model of Clark et al. (1980) was challenged by Jones (1987), who cautioned that the quality of the paleomagnetic data set varies widely, from samples analysed with full stepwise demagnetisation and six-spin measurements to no demagnetisation and only one-spin measurements. By using only those cores that had been demagnetised up to 50 Oe and that could be placed into Clark’s lithostratigraphic units, 14 cores remained for which inclinations were calculated (Jones, 1987). Jones added data from three cores and used inclination data from these 17 cores to propose that the “oldest continuously accumulating sediment (i.e. not found below a hiatus) recovered from the T-3 platform is approximately 2.5 million years old, and is not Miocene in age as previously interpreted by Clark et al. (1980).” That is, Jones placed unit A at approximately the Matuyama/Gauss boundary, which is about 0.8 Myr younger than Clark’s (1970) estimate (“< 3.32 Myr”; see Clark et al., 1980, p. 18), and about 3 Myr younger than Clark’s et al. (1980) estimate (5.62 Ma), of unit A in core FL 224. Later on, Clark et al. (2000) followed Jones’ age model, in using an age of 2.6 Ma for unit A. Nevertheless, Jones’ revised age model implies that the oldest Neogene sediment in the T-3 cores is of late Middle Pliocene age. His age model also implies that the average sedimentation rate is approximately 0.15 cm/ka, which is about two to three times higher than that proposed by

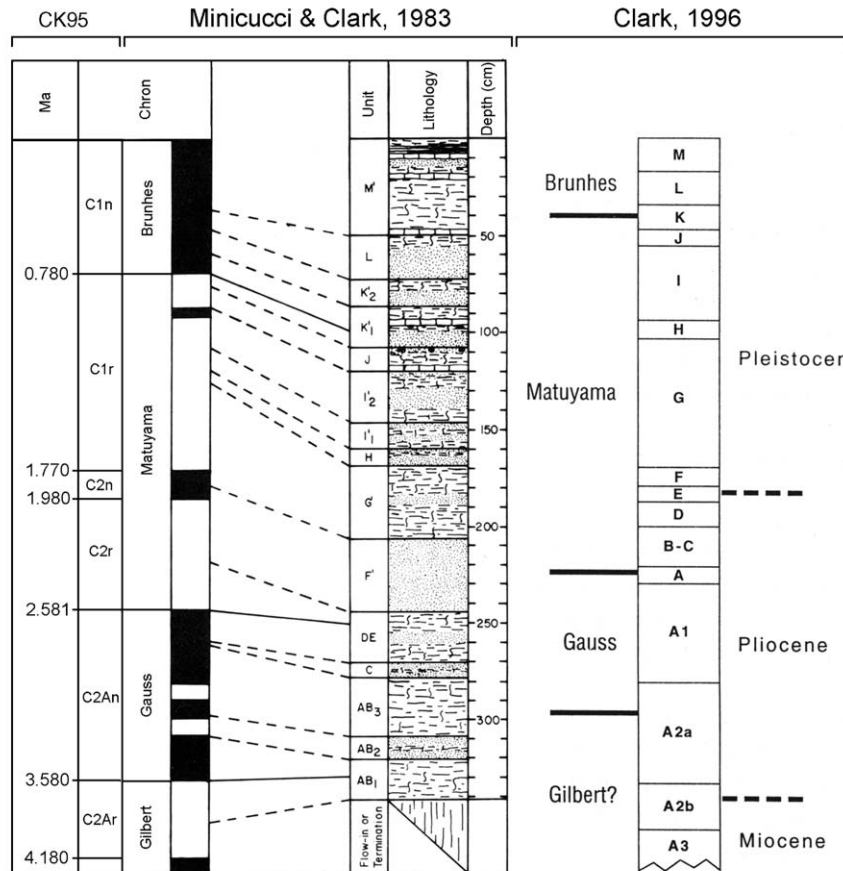


Fig. 1. Correlations between the GPTS and lithostratigraphic units A–M of Clark et al. (1980). Modified from Minicucci and Clark (1983), which is largely similar to that of Clark et al. (1980, Fig. 2), and Clark (1996). Notice development of interpretation of the correlations. Ages (Ma) and chron designations are from Cande and Kent (1995).

Clark et al. (1980); however, this revised age model does not oppose the view that low sedimentation rates persisted during the Late Pliocene and Pleistocene in the central Arctic Ocean. According to this view, large areas in the central Arctic Ocean consequently were sediment starved during Plio–Pleistocene times, yielding sedimentation rates that are comparable to those of the Cenozoic brown pelagic clay facies of the deep Pacific Ocean (Doyle and Riedel, 1979).

The age model of Clark et al. (1980) was subsequently discussed by Darby et al. (1989). They remarked that Clark's model was based on approximately 7500 spinner magnetometer measurements on 146 of the 580 T-3 cores, and that none of these paleomagnetic data was published. Inclination, declination, and intensity values were not calculated for any of these 7500 samples. In their discussion about the quality of the paleomagnetic data of the T-3 cores, Darby and others remark that "in order to obtain as much paleomagnetic data as possible from many cores shortcuts were made. It was reasoned that since these cores were collected from such high latitudes, the inclination vectors would be nearly

straight up or down. Therefore, just the sign of the in-phase value from a one-spin measurement would be sufficient to determine if a sample was of normal or reversed polarity." Even if the quality of the spinner measurements of these 146 T-3 cores appears to be justifiably described as ambiguous, the application of the paleomagnetic method on Arctic Ocean sediment cores more than two decades ago would not have resolved the chronostratigraphic ambiguities in the raised cores. The reason for this is that excursions of short durations within the Brunhes Chron complicated the interpretation of the paleomagnetic stratigraphy, as discussed below.

3.2. The *cm-scale scenario*

Arguments for higher Arctic sedimentation rates appear early in the literature, e.g. 0.7 cm/ka from ^{14}C dating of the uppermost ~10 cm of core T3-67-11 from the Mendeleev Ridge (van Donk and Mathieu, 1969). Later on, both scenarios have been suggested for this core. Herman (1974) suggested that the 210 cm level in

core T3-67-11 is referable to the Mammoth Subchron within the Gauss Chron, about 3.23 Ma (modern estimate), based on paleomagnetic data presented by Hunkins et al. (1971). In contrast, Sejrup et al. (1984) argued that the 260 cm level in this core is younger than 0.3 Ma, based on amino acid epimerisation measurements of foraminiferal tests and on the composition of benthic foraminiferal assemblages: “biostratigraphy (...) indicate a late Quaternary rather than a Pliocene age”. Herman’s and Sejrup’s age estimates differ by well over one order of magnitude, thus resulting in a corresponding major difference in sedimentation rate estimates.

Another study on amino acid epimerisation in planktic foraminifers resulted in an estimate of about 0.1 cm/ka in a core from the Alpha Ridge (Macko and Aksu, 1986). Obviously there is room for systematic studies, involving more than these two cores, of amino acid epimerisation of foraminifers from various parts of the central Arctic Ocean.

Many studies of Arctic Ocean sediment cores argue for sedimentation rates that are on the order of the cm-scale level, rather than mm-scale. Along a transect across the Amerasia Basin, Darby et al. (1997) noticed that “deposition rates are generally less than 0.5 cm/ka for glacial regimes, greater than this for deglacial regimes and greater than 1–2 cm/ka for interglacial regimes” using radiocarbon dating of box-core material.

Most data sets reporting cm/ka-scale rates refer to the Eurasia Basin. Markussen et al. (1985) determined Holocene and Last Glacial Maximum sedimentation rates of about 2.0 cm/ka in two cores from the north-western flank of the Gakkel Ridge using the oxygen isotope method. Baumann (1990, Fig. 2c) observed single peak occurrences of the calcareous nannofossil genus *Gephyrocapsa* spp. in two cores from the northern Nansen Basin and the Gakkel Ridge, “and because of the presence of *E. huxleyi*, they should both represent oxygen isotope stage 5.” As these peaks occurred at ca 123 cm and 330 cm core depth, respectively, sedimentation rates of about 1 cm/ka and 3 cm/ka, respectively, are derived for these two cores. Gard (1993, Table 1) used nannofossil biostratigraphy to estimate Holocene sedimentation rates in cores from the Nansen Basin (5.1 cm/ka, $N = 14$), the Gakkel Ridge (3.0 cm/ka, $N = 19$), the Amundsen Basin (1.8 cm/ka, $N = 16$), the Lomonosov Ridge (1.5 cm/ka, $N = 16$), and the Makarov Basin (1.4 cm/ka, $N = 5$). The average of all these 70 Holocene estimates is 2.6 cm/ka. In one core, PS2208-2 from the northern Nansen Basin, Gard (1993, Fig. 5) observed peak abundances of *Gephyrocapsa* spp. co-occurring with *E. huxleyi* at about 400 cm core depth, and concluded that “This core has a high sedimentation rate, ~4.4 cm/ka, for the last glacial and at least 1.4 cm/ka for the last interglacial.” Stein et al. (1994) estimated the

sedimentation rate during MIS 1, using stable isotopes and AMS ^{14}C datings, in 18 of the 70 cores that Gard investigated. Stein’s data cover the identical set of basins and ridges, yielding an average rate of 1.0 cm/ka in these 18 cores. Schneider et al. (1996) analysed six cores from the eastern Arctic Ocean using paleomagnetic stratigraphy and AMS ^{14}C datings. Five of the six cores show rates > 1.0 cm/ka, including two cores showing rates between 3.0 and 4.0 cm/ka. The sixth core, retrieved from the Morris Jesup Rise, shows a rate < 0.6 cm/ka. Nevertheless, Schneider and others concluded “that sedimentation rates on the Eurasian side of the Lomonosov Ridge can be variable and are much higher than the few mm/10³ yr rates in many previous studies of Arctic sediments from the Canada Basin.”

Nowaczyk et al. (1994) placed MIS 5e at 345–370 cm depth in core PS2212-3 from the eastern slope of the Yermak Plateau, implying a rate of about 2.7 cm/ka. Aldahan et al. (2000) analysed ^{10}Be concentrations in one of the cores (PS2208-2 from the western Nansen Basin) studied also by Gard (1993) and Schneider et al. (1996). Aldahan concludes that the sedimentation rate varies from 2.4 cm/ka to 5.0 cm/ka between MIS 1 and MIS 9. Jakobsson et al. (2000a) analysed a 722 cm long piston core (96/12-1pc) from the crest of the Lomonosov Ridge using nannofossil biostratigraphy, paleomagnetism, and cyclic variability in colour and manganese content. The upper 193 cm of the core, through MIS 4, was interpreted to have a rate of 2.8 cm/ka. The rates in the remaining lower part (through MIS 21.5) were estimated to vary between 0.2 and 1.6 cm/ka, with an average of 0.5 cm/ka. In order to further evaluate the age model for the Lomonosov Ridge sediments, Jakobsson (2002) applied an absolute dating method, Optically Stimulated Luminescence (OSL), on a 4 m long core from the ridge crest. The OSL results agree with the age model established for the nearby-located core 96/12-1pc and, thus, support cm/ka-scale sedimentation rates.

In the Makarov Basin, Nowaczyk et al. (2001) used paleomagnetic data in two cores and proposed two possible age models, one based on correlation of paleointensity records between the Makarov Basin core and North Atlantic ODP Site 983, and the other on correlation to North Pacific ODP Site 1010. The two models are compatible down to 2 m core depth in showing an average rate of about 4.0 cm/ka (Nowaczyk et al., 2001, Fig. 17). Below that depth, to about 12 m core depth, the former age model yields an average sedimentation rate of ~5.0 cm/ka whereas the latter yields a rate of ~1.0 cm/ka. In the southern Canada Basin, the “average net accumulation rate of the mixed sequence of turbidites and thin pelagite interbeds in the cores is about 1.2 m/1000 yr” [= 120 cm/ka] (Grantz et al., 1996). Recently, Svindland and Vorren (2002)

applied Jakobsson's et al. (2000a) age model on two cores from the Amundsen Basin, resulting in sedimentation rates of 5.9 cm/ka (North Pole core) and 24.7 cm/ka over the past 17 ka.

Key cores representative of both sedimentation rate scenarios (mm/ka versus cm/ka) are listed in Table 1 and plotted in Fig. 2.

4. Sedimentation rates from seismic reflection and refraction data, and tectonic models of bedrock age

Most of the seismic reflection and refraction data in the Arctic Ocean has been collected from drifting ice stations on which “the direction of the lines is controlled by the whims of nature” (Jackson et al., 1990). Her plots

Table 1
Sedimentation rates (cm/ka) in cores from the central Arctic Ocean

Core	Author	Latitude	Longitude	Depth	cm_ka	Age control
94-PC29	Grantz et al. (2001, Fig. 7)	88.94	138.71	3010	0.04	Top core to 220 cm (“lower Pliocene”) if age is 5.0 Ma; 0.06 cm/ka if age is 4.0 Ma
FL 224	Clark et al. (1980, Fig. 29)	80.46	−158.81	3467	0.05	Top Gauss to top “polarity epoch 5” (= top Chron C3An.1n)
FL 270	Clark et al. (1980, Fig. 30)	83.19	−154.01	3280	0.06	Top core to Brunhes/Matuyama boundary
FL 196	Clark et al. (1984, Fig. 4)	80.56	−171.58	3327	0.06	Top core to Brunhes/Matuyama boundary
T3-67-11	Herman (1974, Fig. 20)	79.58	−172.50	2810	0.06	Top core to middle part of Mammoth Subchron
CESAR 14	Aksu and Mudie (1985, Fig. 2)	85.85	−108.36	1370	0.08	Top core to Gauss/Gilbert boundary
FL 331	Clark et al. (1980, Fig. 30)	84.27	−134.63	2659	0.09	Top core to Brunhes/Matuyama boundary
FL 380	Clark et al. (2000, Fig. 2)	84.63	−128.46	2401	0.09	Top core to unit A assuming linear depth scale in Fig. 2 and that base unit A2 is 345–60 cm = 285 cm
CESAR 103	Aksu and Mudie (1985, Fig. 2)	85.64	−111.12	1585	0.10	Top core to Brunhes/Matuyama boundary
FL 224	Steuerwald et al. (1968, Fig. 1)	80.46	−158.81	3467	0.10	Base Brunhes to top Gauss (base Brunhes of Steuerwald Fig. 1 = top Gauss of Clark et al. (1980, Fig. 29)
FL 228	Clark et al. (1980, Fig. 30)	80.82	−158.82	3632	0.10	Top core to Brunhes/Matuyama boundary
CESAR 102	Macko and Aksu (1986, Fig. 2)	85.63	−111.12	1495	0.11	Top core to Brunhes/Matuyama boundary
FL 435	Clark et al. (1980, Fig. 30)	86.06	−129.54	2272	0.14	Top core to Brunhes/Matuyama boundary
LOREX B-24	Morris et al. (1985, Figs. 3 and 9)	89.08	−168.49	0	0.16	Top core to base unit M inferred at 400 ka (= 427 ka if B/M boundary = 780 ka)
T3-67-12	Witte and Kent (1988, Table 1)	80.35	−173.52	2867	0.16	Top core to base Olduvai
PS51/034-4	Jokat et al. (1999a, Fig. 3)	85.38	−155.46	2071	0.17	Lithostratigraphic unit B/C boundary at 1.9 Ma
PS2185-6	Spielhagen et al. (1997, Fig. 2)	87.53	144.17	1052	0.18	Top core to Gauss/Gilbert boundary
LOREX B-8	Morris et al. (1985, Figs. 2 and 9)	88.50	−167.13	0	0.18	Top core to unit K inferred to hold Brunhes/Matuyama boundary
FL 409	Clark et al. (1980, Fig. 30)	84.46	−127.00	2742	0.19	Top core to Brunhes/Matuyama boundary
92PC-38	Phillips and Grantz (2001, Fig. 10)	75.87	−155.70	1917	0.20	Top core to “initiation of glacial ice-rafting at 2.7 Ma” ^a
T3-67-6	Witte and Kent (1988, Table 1)	79.73	−173.07	2815	0.25	Top core to base Jaramillo
FL 199	Clark et al. (1984, Fig. 2)	80.20	−172.79	2988	0.26	Top core to Brunhes/Matuyama boundary
NWR 5	Poore et al. (1993, Fig. 2)	74.62	−157.88	1089	0.38	Top core to base Jaramillo
PS2178-3/2180-2	Nowaczyk et al. (2001, age model 2)	87.64	156.97	3991	0.54	Paleointensity correlation; composite depth: 1000–1150 cm
96/12-1pc	Jakobsson et al. (2000a, b, Fig. 3)	87.10	144.77	1003	0.72	Top core to Brunhes/Matuyama boundary
Core 4	Phillips and Grantz (1997, Fig. 8)	74.61	−157.40	2430	0.86	Top core to Brunhes/Matuyama boundary; “composite stratigraphic section of cores 4, 5 and 9”
T3-67-11	Sejrup et al. (1984)	79.58	−172.50	2810	0.87	Minimum rate (“260 cm depth...younger than 300 kyr”; amino acid epimerisation and biostratigraphy
PS1527-20	Baumann (1990, Fig. 2c)	86.14	22.06	3780	1.0	Coccolith abundance peak in MIS 5 with <i>E. huxleyi</i>
PS2178-3/2180-2	Nowaczyk et al. (2001, age model 2)	87.64	156.97	3991	1.0	Paleointensity correlation; composite depth: 200–1000 cm

Table 1 (continued)

Core	Author	Latitude	Longitude	Depth	cm/ka	Age control
PS2185-5	Gard (1993, Table 1)	87.53	144.17	1051	1.4	Holocene coccolith data (represents the average Holocene rate on the Lomonosov Ridge)
PS2757-8	Matthiessen et al. (2001, Fig. 9)	81.16	140.20	1230	1.6	Dinoflagellate cyst stratigraphy correlated to MIS 5/6 boundary
PS2195-4	Gard (1993, Table 1)	86.23	9.59	3873	1.7	Holocene coccolith data (represents the average Holocene rate in the Amundsen Basin)
FRAM-I/4	Markussen et al. (1985, Fig. 4)	84.49	−8.97	3820	2.0	Oxygen isotopes from top core through Termination 1A
FRAM-I/7	Markussen et al. (1985, Fig. 4)	83.87	−6.95	2990	2.0	Oxygen isotopes from top core through Termination 1A; 3.5 cm during MIS 2
PS2192-1	Gard (1993, Table 1)	88.26	9.88	4375	2.1	Holocene coccolith data
PS2163-2	Gard (1993, Table 1)	86.24	59.23	3047	2.9	Holocene coccolith data (represents the average Holocene rate on the Gakkel Ridge)
PS1529-8	Baumann (1990, Fig. 2c)	85.36	21.74	2917	3.0	Coccolith abundance peak in MIS 5 with <i>E. huxleyi</i>
PS2208-2	Aldahan et al. (2000, Fig. 7)	83.65	4.67	3682	3.0	¹⁰ Be dating through MIS 9
PS2178-3/ 2180-2	Nowaczyk et al. (2001, age model 1)	88.05	159.17	4009	3.8	Paleointensity correlation; composite depth: 200–1250 cm
PS2178-3/ 2180-2	Nowaczyk et al. (2001, age model 1 + 2)	88.05	159.17	4009	4.0	Paleointensity correlation; composite depth: 0–200 cm
PS2208-2	Gard (1993, Fig. 5)	83.65	4.67	3682	4.0	Coccolith abundance peak in MIS 5 with <i>E. huxleyi</i>
PS2161-2	Gard (1993, Table 1)	85.45	44.39	4005	5.0	Holocene coccolith data (represents the average Holocene rate in the Nansen Basin)
PS2138-1	Matthiessen et al. (2001, Fig. 3)	81.54	30.43	995	5.0	Linear sedimentation rate from first used ¹⁴ C date at 65 cm (12,999 BP) ^a
PS2190-1	Svindland and Vorren (2002)	90.00		4275	5.9	Adopting Jakobsson's et al. (2000a) age model for the past 17 ka
PS2176-3	Svindland and Vorren (2002)	87.77	108.39	4364	24.7	Adopting Jakobsson's et al. (2000a) age model for the past 17 ka
P1-88-AR (PC-10)	Grantz et al. (1996, Fig. 8)	74.73	−156.14	3899	120.0	Top core to 847 cm; linear regression of seven radiocarbon ages ($r = 0.9913$)

In the four cases where two cores occur in one row, core designations in bold face refer to the core that shows longitude, latitude and water depth. A few cores are listed twice, when published estimates of sedimentation rates differ widely. Most sedimentation rate values (cm/ka) are approximative because core depths of age control points are predominantly estimated from published figures.

^a¹⁴C dates further down core show larger sedimentation rates through MIS 2 in core PS2138-1.

of all available seismic reflection and refraction lines through 1986 emphasises the sparseness of Arctic Ocean seismic data. New sets of airgun data were acquired after 1990 as a result of successful icebreaker expeditions into the central Arctic Ocean: 1991 (*Oden* and *Polarstern*, the first conventionally powered surface ships to reach the North Pole, but the 5th and 6th ships at the North Pole); 1993 (*Polar Star*); 1994 (*Louis St. Laurent* and *Polar Sea*, the 16th and 17th ships at the North Pole); 1996 (*Oden*, 23rd ship at the North Pole); 1998 (*Arktika* and *Polarstern*); 2001 (*Oden*, 33rd ship at the North Pole); and 2001 (*Healy* and *Polarstern*, 36th and 37th ships at the North Pole). The direction of lines in these efforts are also heavily influenced “by the whims of nature”, with the result that the seismic data are not acquired in pre-defined, systematic trackline surveys. When these icebreaker lines are added to those collected from drifting stations, we still possess only unevenly distributed glimpses of seismic information from the deep Arctic

Ocean. Cross-lines are rare, making interpretations of three-dimensional geological structures difficult.

Estimates of sediment thickness based on seismic data include the compilations by Kristoffersen (1990, Eurasia Basin), by Grantz et al. (1990, Canada Basin), and by Weber and Sweeney (1990, Lomonosov, Alpha and Mendeleev ridges, Makarov Basin). Seismic reflection and refraction data available before 1990 were summarised in a map showing sedimentary thickness for the entire Arctic Ocean (Jackson and Oakey, 1990), incorporating data also from Soviet sources. The isopach sediment thickness curves from this map are shown in Fig. 2.

During the 1991 icebreaker expedition, seismic reflection and refraction data were collected along two lines crossing the Lomonosov Ridge (87–88°N/130–160°E), and along a profile across the Eurasia Basin (Jokat et al., 1992, 1995). They demonstrated that almost 500 m of sediments have been deposited on the top of the

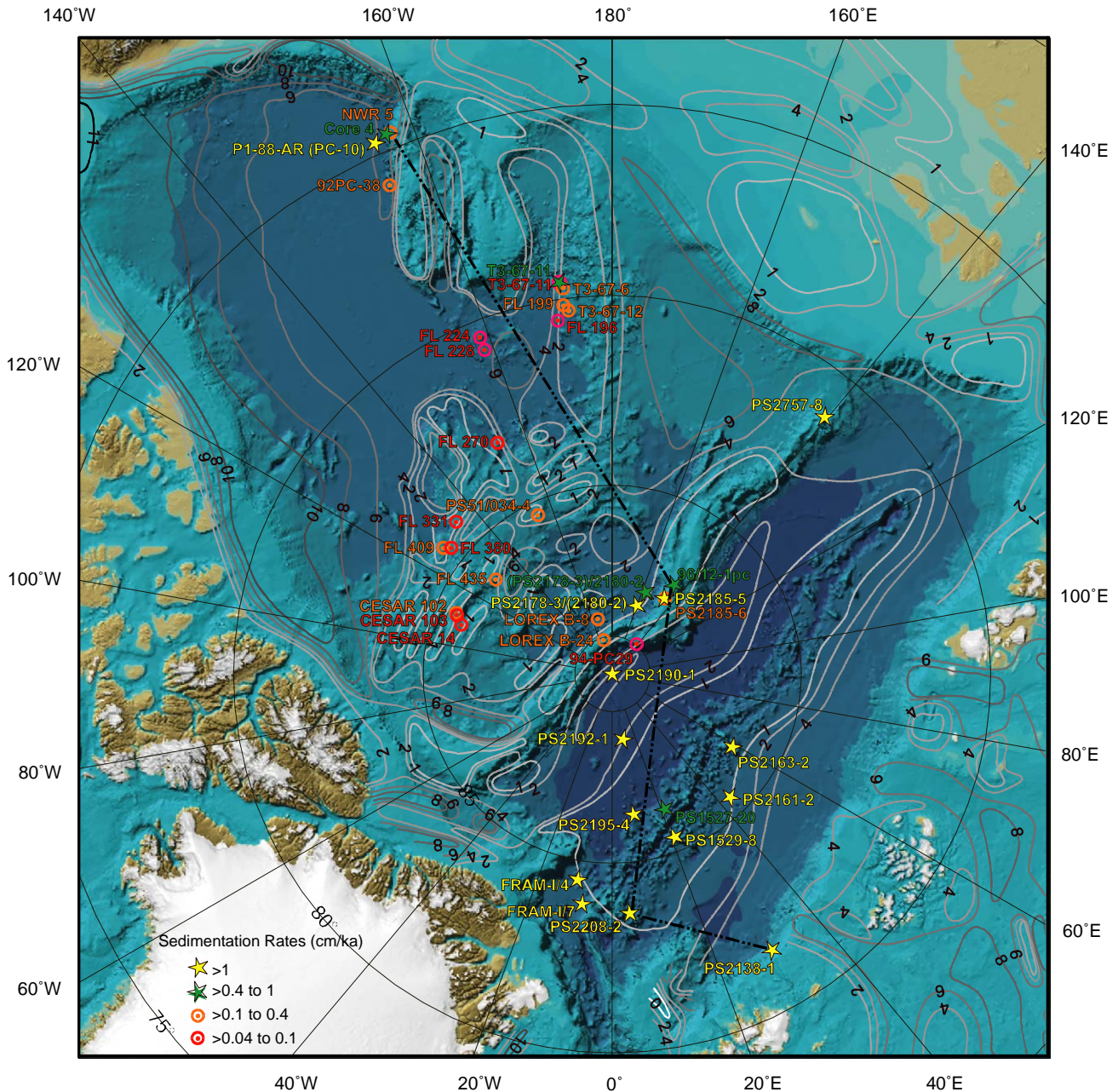


Fig. 2. Locations of sediment cores discussed in this study and their inferred sedimentation rates from previous studies (for listing of cores see Table 1). The bathymetry is portrayed by the International Bathymetric Chart of the Arctic Ocean (IBCAO) (see www.ngdc.noaa.gov/mgg/bathymetry/arctic/arctic.html and Jakobsson et al. (2000b)). Contour lines represent sediment thickness isopachs in km (from Jackson and Oakey, 1990). Transect of four cores from the Barents slope (PS2138-1), via the Gakkel Ridge (PS1529-3) and the Lomonosov Ridge (96/12-1pc), to the Northwind Ridge (NWR 5), is connected by thick black stippled line. Basis for correlation is presented in Figs. 5 and 6.

Lomonosov Ridge since the subsidence of the ridge below sea-level at about 50 Ma, implying an average sedimentation rate of about 1.0 cm/ka since the Early Eocene.

The Gakkel Ridge is the active spreading ridge in the Eurasia Basin, bisecting it into two sub-basins, the Amundsen Basin towards the Lomonosov Ridge and the Nansen Basin towards the Eurasian margin, which

show a symmetrical progression of seafloor magnetic anomalies away from the spreading ridge (Kristoffersen, 1990 and references therein). Anomaly 25 (~56 Ma) of the latest Paleocene is the oldest identified magnetic lineation in both sub-basins (Kristoffersen, 1990). This tectonic model was used by Jokat et al. (1995, Figs. 10–12) when estimating sediment thickness on identified seafloor magnetic anomalies in the Amundsen Basin,

resulting in an average sedimentation rate of 1.5 cm/ka between the Recent and 36 Ma (Anomaly 16), 5.4 cm/ka between 39 (Anomaly 18) and 46 Ma (Anomaly 21), 8.6 cm/ka between 46 and 49 Ma (Anomaly 22), and 14.0 cm/ka between 49 and 53 Ma (Anomaly 24). The Nansen Basin received more sediments than the Amundsen Basin, seen also in its 300–700 m shallower abyssal plain (Kristoffersen, 1990; see also sediment isopach lines in Fig. 2), implying higher sedimentation rates than in the Amundsen Basin. This difference in sedimentation rates has been suggested to be caused by larger input of terrestrial sediment to the Nansen Basin because over most of its length the Amundsen Basin is isolated from the Eurasia continental margin by the Gakkel Ridge (Johnson, 1969). Elverhøi et al. (1998) conclude that the dominant Quaternary sediment supply to the Nansen Basin was derived via glacial erosion from the Barents–Kara shelf. An average sedimentation rate of 3.0 cm/ka since the “post mid-Oligocene” has been suggested for the abyssal plain of the western Nansen Basin (Kristoffersen and Husebye, 1985).

Isopach lines showing sedimentary thickness in the southern Canada Basin yield values ranging from about 6 km at 3.8 km water depth near the Northwind Ridge to 12 km at 2 km water depth near the Mackenzie delta (Grantz et al., 1990). The opening and formation of the Canada Basin is considered to have occurred during the Cretaceous (Grantz et al., 1990; Lawver and Scotese, 1990), beginning in the Hauterivian (~130 Ma) and ending by middle Aptian time (~110 Ma) (Jakobsson et al., 2003a). By using the old end-member of this age range (130 Ma), a minimum average sedimentation rate of 4.6 cm/ka is obtained from where the total sediment thickness is 6 km and 9.2 cm/ka from where the sediment thickness is 12 km.

The crest and southern flank of the Alpha Ridge carry a sediment drape that is at least 1 km thick according to reflection seismic data collected from the T-3 Ice Island (Hall, 1979, Figs. 6 and 7). More recently, multi-channel seismic profiles (MCS) were collected from an icebreaker along the strike of the Alpha Ridge, showing a rather constant sediment thickness of 800–1200 m (Jokat et al., 1999a, b; Jokat, 2003). The Alpha Ridge is considered to be broadly contemporary with Canada Basin seafloor formation, sometime between 120 and 80 Ma (Sweeney, 1985; Weber and Sweeney, 1990). By using averages for sediment thickness (1000 m) and ridge age (100 Ma), the sedimentation rate is estimated to 1.0 cm/ka on the Alpha Ridge along these MCS profiles. A piece of basalt that was dredged from the Alpha Ridge and dated to 82 Ma (Jokat, 2003) suggests that the average sedimentation rate ranges between 1.0 cm/ka (800 m sediment thickness) and 1.5 cm/ka (1200 m sediment thickness), if assuming that this basalt represents the age of the underlying Alpha Ridge bedrock.

In summary, all longer-term sedimentation rates estimated from seismic reflection and refraction data, and current bedrock age models, are on the order of cm/ka. This applies to both abyssal plains and ridges, except in those cases where obvious erosion has biased the sediment thickness.

5. The heart of the problem: dating Arctic Ocean sediment cores accurately

If sediment cores raised from the seafloor of the central Arctic Ocean could be dated and correlated accurately using a combination of absolute and relative dating methods, the sedimentation rate problem addressed here, with two competing rate scenarios, would not exist. Below follows a review of the key characteristics of the most common methods that have been employed to establish age/depth relationships in Arctic Ocean sediment cores. These methods include biostratigraphy, magnetostratigraphy, oxygen isotopes, and counts of lithological/climatic cycles.

5.1. Biostratigraphic data

Sediment cores largely composed of marine microfossils with continuously occurring and diversified assemblages are well suited for highly resolved biostratigraphic work. For dating purposes, biostratigraphic events must be accurately calibrated to an independent timescale reflecting, as accurately as possible, the true progress of time. Magnetostratigraphy is a key technique for age calibration of Cenozoic marine biostratigraphic events (e.g. Berggren et al., 1985). The introduction of orbitally tuned timescales based on cyclostratigraphy resulted in huge improvements of age calibrations of many bio-events (e.g. Shackleton et al., 1990, 1995, 1999; Hilgen, 1991; Backman and Raffi, 1997), chiefly among the calcareous and biosiliceous groups. Planktic foraminifers, calcareous nannofossils, radiolarians and diatoms therefore are key groups for dating of marine sediments, because they are comparatively well calibrated to independent timescales and because other dating tools are often not applicable. In cases where magneto- and cyclostratigraphies are available, these stratigraphies still depend on biostratigraphy for identification of polarity zones or cycle numbers.

These pre-requisites for accurate biostratigraphic work are commonly encountered in low to mid-latitude marine environments. Approaching northern high latitudes, the taxonomic diversity decreases with increasing latitude. Biostratigraphic marker events that are taxonomically well defined and firmly calibrated to the GPTS or the astronomical timescale occur rarely in Arctic Ocean cores. Biosiliceous groups are not preserved in upper Cenozoic cores. Calcareous faunas and

floras are taxonomically impoverished and occur discontinuously in the cores, commonly only in the upper few meters of the cores. The forms that are present are often long-ranging, such as the planktic foraminifer *Neogloboquadrina pachyderma* (sinistral). This species, completely dominating Arctic Ocean foraminiferal assemblages in most cores, has its evolutionary appearance during the early Late Miocene (Kennett and Srinivasan, 1983) at approximately 9 Ma (Berggren et al., 1995). A recent study suggests, however, that the modern sinistrally coiled variety of *N. pachyderma* appeared at ca 1 Ma, and that this form differs morphologically and ecologically from its early Pleistocene and Pliocene predecessors (Kucera and Kennett, 2002). Its first appearance and subsequent morphologic evolution appear to have been synchronous in the North Pacific and North Atlantic, implying the “existence of trans-Arctic gene flow.” (Kucera and Kennett, 2002). These new findings have not yet been applied to Arctic Ocean planktic foraminiferal assemblages, but hold the promise of helping to constrain age/depth relationships in Arctic cores.

Presence of the nannofossil species *Emiliana huxleyi* is one of the few marker species providing accurate age information that have been observed in the Arctic Ocean. Its first evolutionary appearance is dated to 0.26 Ma (Thierstein et al., 1977), and it has been observed solely in the Holocene and the penultimate interglacial in Arctic cores (Baumann, 1990; Gard, 1993; Jakobsson et al., 2001). Still, the discontinuous occurrence and reduced diversity of calcareous faunas and floras introduce uncertainties when interpreting their stratigraphic distribution: Are observed distributions caused by genuine evolutionary appearances or extinctions, or do they reflect preservational or paleoecologic bias?

For various reasons the use of other microfossil groups for biostratigraphic work in Arctic Ocean sediments, such as benthic foraminifers, dinocysts, ostracodes, pollen and spores, appears ambiguous as accurate age indicators. First, the taxonomy is still under development for some groups (e.g. dinocysts). Second, their stratigraphic ranges in Arctic Ocean sediments are insufficiently known, implying that the ranges are likely to change as new material becomes available. Third, bio-events among these groups still appear to be inadequately calibrated to independent timescales. Fourth, biostratigraphic events indicated by pollen and spores in Arctic Ocean cores (e.g. Aksu and Mudie, 1985) chiefly appear to reflect climate driven biogeographic migration events on surrounding land masses, rather than evolutionary emergences or extinctions, making it difficult to judge the precise biochronologic value of presence/absence of species of pollen and spores in cores raised from the central Arctic Ocean.

5.2. The oxygen isotope method

The use of the stable isotope method is constrained by the discontinuous and limited distribution of foraminiferal calcite in Arctic Ocean sediments. Moreover, reduced surface water salinities, resulting from voluminous riverine discharge and meltwater events, influence the oxygen isotope records generated from planktic foraminifers (e.g. Aksu et al., 1988; Stein et al., 1994; Nørgaard-Pedersen et al., 1998). These two characteristics hamper the usefulness of the oxygen isotope method because continuous records through entire cores cannot be established, and because curves generated from intervals containing foraminiferal calcite are blurred by salinity signals (e.g. Stein et al., 1994, Figs. 5 and 6). Therefore correlation of oxygen isotope curves via pattern recognition between Arctic Ocean cores and low and middle latitude oxygen isotope records in general do not yield reliable age information. The extraction of oxygen isotopes from different materials such as fish-teeth apatite presumably has future potential for reconstructing paleoenvironmental conditions in the Arctic Ocean.

5.3. Paleomagnetic age models in the Arctic Ocean: reversals versus excursions

Paleomagnetic age models are based on interpretation of changes in measured intervals of uniform geomagnetic polarity directions that are caused by time-dependent changes in Earth's magnetic field. The measured polarity pattern in a sediment core, commonly plotted as black and white stripes, does not contain any direct information on the age and the polarity changes may represent either full polarity reversals which are followed by longer time intervals of predominantly one polarity direction (chrons or subchrons, see Cande and Kent, 1992), or polarity excursions of shorter duration (Fig. 3). The duration of a chron is typically on the order of several hundred thousand years, whereas excursions may last less than five thousand years (Jacobs, 1994). Therefore it is crucial to acquire independent age control to guide the interpretation of the paleomagnetic polarity pattern in order to establish an accurate chronology. Central Arctic Ocean sediment cores by-and-large suffer from the lack of such independent age control, forcing scientists to rely on interpretations of paleomagnetic polarity patterns without guidance from independent age control.

The first chronologies of sediment cores retrieved from the Amerasia Basin were based on the assumption that zones with negative inclination represented genuine polarity reversals. The first encountered down-core zone with negative inclination was interpreted to be the Brunhes/Matuyama boundary, presently dated to 780 kyr (Shackleton et al., 1990). This approach yielded

mm-scale Plio–Pleistocene sedimentation rates (Steuerwald et al., 1968; Clark, 1970; Hunkins et al., 1971; Herman, 1974; Clark et al., 1980, 1984, 2000; Minicucci and Clark, 1983; Aksu, 1985; Aksu et al., 1988; Witte and Kent, 1988; Poore et al., 1993), and implies that the sediment supply to the Amerasia Basin is best described in terms of starvation during the past 5 Ma.

The first report of a chronostratigraphically confined geomagnetic excursion in marine sediments appeared

during the late 1960s (Smith and Foster, 1969). But the reality of excursions as genuine geomagnetic features remained a matter of dispute for decades (Verosub, 1975, 1982), and only recently have excursions achieved general acceptance (Langereis et al., 1997; Gubbins, 1999). The assumption of early studies that intervals with negative inclinations in Arctic cores represent genuine polarity reversals simply reflects the history of science in this field. Consequently, geomagnetic excursions have not, until recently, been considered an alternative to polarity reversals when interpreting paleomagnetic data in sediment cores. The absence of a commonly accepted standard geomagnetic excursion timescale has also contributed to reducing the usefulness of excursions as age indicators.

Geomagnetic excursions are commonly observed in sediment cores from the Arctic Ocean and the sub-polar North Atlantic (Sejrup et al., 1984; Løvlie et al., 1986; Bleil and Gard, 1989; Nowaczyk and Baumann, 1992; Frederichs, 1995; Nowaczyk et al., 2001). Thus, if published chronologies based on paleomagnetic records have been incorrectly interpreted as reversal boundaries rather than excursions within the Brunhes Chron, it follows that the resulting estimates of sedimentation rates must be off by at least one order of magnitude. A comparison of the reversal boundary alternative versus the excursion alternative proposed by Frederichs (1995) based on core PS2185-6 from the crest of the Lomonosov Ridge resulted in significant differences in age estimates (Fig. 4).

In addition to assigning short reversed polarity intervals with excursions or sub-chrons, a recurrent observation is the absence or incomplete records of geomagnetic excursions in marine cores within the Brunhes chron. Geomagnetic excursions were rapid, high-amplitude directional variations of the geomagnetic field, associated with low intensities (Jacobs, 1994).

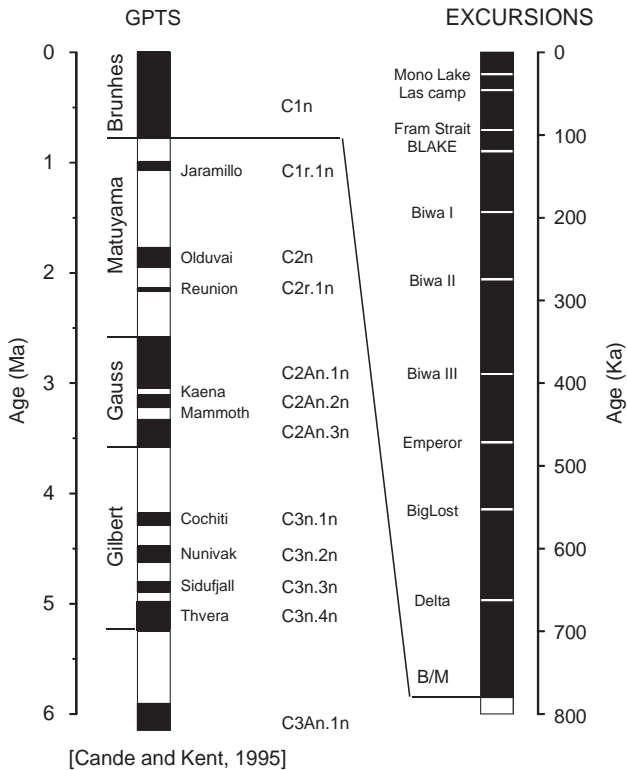


Fig. 3. GPTS (Cande and Kent, 1992) and established excursions within the Brunhes Chron (Langereis et al., 1997).

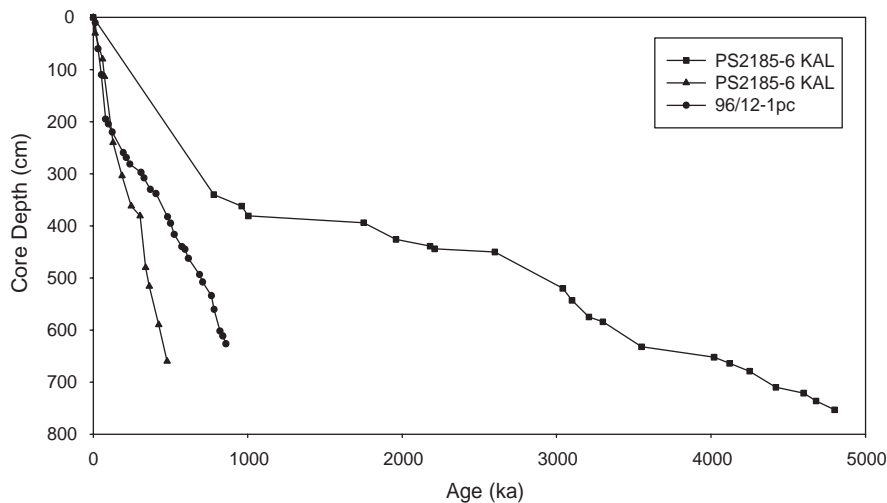


Fig. 4. Two alternative age-depth relationships for core PS2185-6 KAL vs. core 96/12-1pc. The excursion scenario (Frederichs, 1995) for core PS2185-6 is plotted with triangles and the true reversal boundary scenario (Frederichs, 1995; Spielhagen et al., 1997) with squares.

The absence of paleomagnetic excursions in sediments covering adequate time intervals, can be attributed to factors controlling the preservation of the time-signal: e.g. variation in sediment accumulation, intermittent bioturbation (Watkins, 1968) or the erasing of the paleomagnetic signal by post-depositional realignment of magnetic grains. The significance of variations in accumulation is difficult to assess because the produced hiatuses/compression only cover a time interval on the order of the duration of the excursion in question. The duration of excursions is poorly known except for a few cases: the Blake excursion has an estimated duration of ~5 ka (Jakobs, 1994), the Laschamp excursions lasted ~2 ka (Nowaczyk and Knies, 2000), and the Lake Mono excursion lasted ~1.5 ka (Nowaczyk and Knies, 2000). There is presently no general method that may convey such detailed information about variations in sediment accumulation of Arctic sedimentary cores. The action of intermittent bioturbation also requires independent observations that are not generally available. Post-depositional realignment of magnetic grains has recently been demonstrated to be an intensity-dependent process (Coe and Liddicoat, 1994; Løvlie, 1994), implying that paleomagnetic signals imposed in low-intensity geomagnetic fields may be wiped out and replaced by succeeding geomagnetic directions associated with higher field. This process is not very well investigated, but it is likely that the important factors may be grain-size distribution and degree of sorting of the sediment (Payne and Verosub, 1982).

The youngest excursion recorded in the core investigated by Jakobsson et al. (2001) was identified as Biwa II occurring at 280 cm depth. There is no evidence for major hiatuses above this excursion and it may thus be inferred that records of the Blake, Laschamp and Mono Lake excursions have been wiped out. The process(es) erasing the inferred excursions have not been established. However, the drop in grain size distribution (> 63 µm) occurring at 260 cm depth (from ca 30% to ca 10%), may imply post-depositional re-alignment of magnetic grains in the coarser section of the core, while the lower, more fine-grained section has retained records of excursions.

5.4. Lithological and climatic cycles, unconformities and condensation

Lithological cycles are pervasive in central Arctic Ocean sediment cores (Clark et al., 1980, Fig. 9). Grain size, colour and the degree of mottling are key parameters used to describe the cycles, which are consistently interpreted in terms of glacial-interglacial cycles (e.g. Darby et al., 1989; Clark, 1990; Phillips and Grantz, 1997; Jakobsson et al., 2000a). In a model of a typical lithostratigraphic cycle on the Northwind Ridge, Phillips and Grantz (1997, Fig. 6) illustrate the

characteristics of a single depositional cycle, composed of two parts, one formed during interglacial and the other during glacial conditions.

Clark et al. (1980) suggest that only a few of the several hundred cores investigated were compromised by unconformities, implying strong condensation for the remaining cores. Well over 50 glacial/interglacial couplets (Tiedemann et al., 1994) occurred over the critical time interval encompassed by Clark's 13 lithostratigraphic units if the age model of Jones (1987) for Clark's unit A (upper Gauss) is adopted. If averaged over the entire interval, each lithologic unit has a duration of 200 kyr (13 units deposited over 2.60 Myr). If Clark's 1980 age model is applied, each unit has an average duration of 500 kyr (13 units deposited over 6.5 Myr). None of the well-known Plio–Pleistocene glacial/interglacial couplets (e.g. Shackleton et al., 1990; Tiedemann et al., 1994) are resolved in this litho- and chronostratigraphic model (Clark et al., 1980, Figs. 9 and 29; Clark, 1990, Figs. 5 and 6).

Unit K is considered to hold the Matuyama/Brunhes boundary (Clark et al., 1980). The units represented by the upper half of unit K and the two overlying lithologic units (L and M) thus have an average duration of 312 kyr (2.5 units deposited over 0.78 Myr). The nine Pleistocene glacial/interglacial couplets that occurred during this time interval (Shackleton et al., 1990) are thus not resolved in Clark's litho- and chronostratigraphic model.

Similarly, unit K is considered to have a duration of 264 kyr (282 kyr when adopting Shackleton's et al., 1990, timescale for the Brunhes Chron) and to encompass the interval from basal MIS 15 through basal MIS 21 (Clark et al., 1980, Table 3, Fig. 67). Their model therefore implies that the glacial/interglacial cyclicity occurring during the formation of these three glacial/interglacial couplets did not result in any discernable variability in lithology, as unit K is described as a virtually homogenous bioturbated silty lutite (Clark et al., 1980, Fig. 9).

Phillips and Grantz (1997, Figs. 3 and 8) presented a composite, less condensed, stratigraphic section from the Northwind Ridge, in which they combined Clark's traditional stratigraphy with a new set of lithostratigraphic cycles, each being composed of an interglacial/glacial couplet correlated to the standard marine oxygen isotope stages through stage 22/23. Phillips and Grantz estimated each couplet to have an approximate duration of 93.5 kyr throughout the Brunhes and about 105 kyr during the late Matuyama, concluding that "there was no large change in the average duration of glacial/interglacial cycles across the late Matuyama-Brunhes transition in the Amerasia Basin."

Core 96/12-1pc from the Lomonosov Ridge showed that cyclically occurring medium to dark brown units were coloured by enhanced concentrations of manga-

nese related to interglacial conditions. These cycles were correlated to low-latitude oxygen isotope stages (Jakobsson et al., 2000a). Subsequently, this age model has been confirmed through MIS 6 by OSL dating (Jakobsson et al., 2003b). Moreover, this age model yielded much higher sedimentation rates than in most earlier models, and indicates that intervals of negative inclination in this Arctic core represent excursions within the Brunhes Chron.

6. Estimates of present and past sediment flux

Sea-ice rafting is the major transport mechanism today that delivers clastic sediments to the central Arctic Ocean (Pfirman et al., 1990; Nürnberg et al., 1994). This process appears to have been active at least as far back in time as the records of most available cores (Clark and Hanson, 1983). Quantitative estimates of present entrainment and transport therefore have the potential to serve as a guide for interpreting Arctic sediment cores, if we assume that today's sediment transport processes show general similarities with those occurring during previous Pleistocene interglacials.

The Laptev Sea has been characterised as the 'ice-factory' of the Arctic Ocean, as this shelf sea is a known locus for ice production. Large amounts of sediments are known to be incorporated into the sea-ice formed on the Laptev Sea shelf (Lindemann et al., 1999). Eicken et al. (2000) studied one such source area near the New Siberian Islands for sediment sea-ice entrainment and dispersal through the Transpolar Drift to the Arctic Basin. By combining field measurements, remote sensing and numerical modeling, they estimated the total export of sea-ice carried sediment to be 18.5×10^6 t for an event in 1994/1995. To emphasise the magnitude of this source alone, Eicken et al. (2000) postulated that if 65–80% of this material would melt out and be distributed over 3×10^6 km² along the Transpolar Drift area, it would contribute to a mass flux of 4–5 g/m² year⁻¹. By assuming a wet bulk sediment density of 1.8 g/cm³, Eicken's flux estimate would yield a sedimentation rate of ~0.2 cm/ka if distributed evenly over 3 million km², an area corresponding to 31% of the Arctic's total area or 67% of the central Arctic Ocean basin (Jakobsson, 2002). The estimate of ~0.2 cm/ka represents the clastic component alone, derived from a single source region. By adding the Arctic's other sediment source regions and input of biogenic components, the value of 0.2 cm/ka is likely to increase several times. However, it is only fair to say that this rate estimate may change substantially to either lower or higher values by changing the seafloor area over which the sediment is assumed to be evenly distributed.

Estimates of the average annual sediment accumulation from another of Arctic's sediment source regions,

the Kara Sea shelf, through Holocene times suggest that about 82% of the initial input of total terrigenous sediment is deposited on the shelf and that about 18% is exported to the interior Arctic Ocean (Stein et al., this issue). In terms of total sediment flux, these 18% correspond to about 35×10^6 t (Stein et al., this issue), implying a sedimentation rate of ~0.4 cm/ka when assuming that the sediments are distributed evenly over 3 million km².

Nørgaard-Pedersen et al. (1998) estimated bulk sediment fluxes in the Holocene central Arctic Ocean to be close to 10 g/m² year⁻¹ from a study using AMS ¹⁴C dating on planktic foraminifera in box cores. These authors also suggest low bulk sediment fluxes during glacial stages MIS 4 and 2, resulting in mm-scale sedimentation rates, presumably caused by dense sea-ice cover in combination with generally low biologic productivity and reduced summer insolation. In one representative box core, PS2185-3, Nørgaard-Pedersen et al. (1998, Fig. 4), show an average sedimentation rates of 0.5 cm/ka from the top of the core to upper MIS 5. Gard's (1993) biostratigraphically derived estimate of the Holocene rate from the same core is 1.4 cm/ka.

Core PS2185-6, which was retrieved from the same sample station as PS2185-3, has been convincingly correlated to core 96/12-1pc (Jakobsson et al., 2001, Fig. 13). Using this correlation and Jakobsson's et al. (2001) age model, we estimate a sedimentation rate of 2.0 cm/ka from the top of core PS2185-6 to the inferred position of upper MIS 5 at ca 160 cm core depth. The four times lower sedimentation rate value obtained by Nørgaard-Pedersen et al. (1998) in core PS2185-3 is possibly explained by their use of a 400 year ¹⁴C reservoir correction, because the ages of glacial deep-water reservoirs may need an order of magnitude higher reservoir correction (Sikes et al., 2000). Clearly, a lid of sea-ice covering the central Arctic Ocean during glacial times may have caused less ventilation and severe, much larger, ¹⁴C reservoir effects in the deep central Arctic Ocean, which could explain the low sedimentation rate obtained from ¹⁴C dating in core PS2185-3.

7. Estimate of the pelagic 'rain' input over the Lomonosov Ridge

Estimates of sedimentation rates from sediment thickness and bedrock age suggest that the Arctic Ocean basin has received such large fluxes of sediments that long-term average sedimentation rates of centimeters per thousand years persisted over tens of millions of years. Short cores retrieved from the abyssal environments indicate the pervasive influence of turbiditic sedimentation, pushing the rates towards higher values (e.g. Svindland and Vorren, 2002), thus masking the input of the true pelagic 'rain' of biogenic, eolian, and

ice-rafted particles. Grantz et al. (1999) compared Holocene pelagic and turbidite sedimentation rates in the Amerasia Basin, concluding that “pelagites were deposited at rates of 1.4–3.2 cm/kyr, and Holocene distal turbidites at a rate of 145 cm/kyr, a range of two orders of magnitude.” Modern estimates based on a plethora of dating techniques applied to sediments from the central parts of the crest of the Lomonosov Ridge also indicate cm/ka-scale rates for the preserved pelagic ‘rain’ component alone (Gard, 1993; Stein et al., 1994; Jakobsson et al., 2000a, 2001, 2002) at coring sites located well over 700 km away from the nearest, Laptev Sea, shelf break. However, as the Laptev Sea margin is approached along the crest of the Lomonosov Ridge, a progressively thicker sediment sequence is observed above the early Paleogene erosional unconformity (Jokat et al., 1992, Fig. 2; Jokat, 1999b, Fig. 9), presumably reflecting the progressive proximity and increased influence of the Lena River discharge source.

The crests on the Lomonosov and the Alpha Ridges are capped by at least 0.5 and 1.0 km of sediments (Hall, 1979; Jokat et al., 1992, 1995; Jokat, 2003), respectively, thus indicating that the input of the pelagic ‘rain’ components (biogenic, eolian, ice-rafted) alone appears to have been sufficiently high to maintain a cm/ka-scale sedimentation on these ridges over tens of millions of years.

8. Correlating stratigraphies from the Amerasia Basin to the Eurasia Basin

Despite all the problems encountered in Arctic Ocean biostratigraphy, compositional and abundance variations among various groups often show coherent patterns over wide distances. Ishman et al. (1996) proposed that systematic variations among benthic foraminiferal assemblages in intermediate to deep (> 1000 m) environments may be more useful for core-correlations than the lithostratigraphic zonation of Clark et al. (1980), simply because the variability among distinctive faunal assemblages yields more easily recognised signals in comparison to the lithostratigraphic variability in sediment texture (i.e. grain size).

Using this approach, it is possible to correlate cores between the Northwind Ridge and the Lomonosov Ridge (Fig. 5), located some 1600 km apart. Cores NWR 5 (Northwind Ridge) and 96/12-1pc (Lomonosov Ridge) have been studied using multi-proxy methods (Poore et al., 1993, 1994; Jakobsson et al., 2000a, 2001), making them valuable for cross-basinal correlation. The two cores were raised from comparable water depths (1089 and 1003 m), which eliminates a bathymetric bias in comparing benthic foraminifers. The proposed correlation is based on maxima or the presence of a few rare foraminiferal species at certain stratigraphic

levels. The zone of abundance of *Bulimina aculeata* is confined to foraminiferal maxima F2-F3 in 96/12-1pc (Jakobsson et al., 2001) and M3-L1 in NWR 5 (Poore et al., 1994). This peak zone has been observed also at the corresponding stratigraphic position in other cores from the Northwind and Mendeleev Ridges (Polyak, 1986; Ishman et al., 1996). Similarly, *Oridorsalis tener* occurs in significant amounts only in F3 and L1 and upcore, whereas *Pullenia* spp. is present only in F7 and K2.

Another useful stratigraphic marker is the boundary between predominantly calcareous and almost exclusively arenaceous faunas that occurs at 287 cm in core 96/12-1pc and at ~445 cm in NWR 5 (Fig. 5). The relative distance of this boundary from the *Pullenia* spp. cluster (F7 and K2) and from the change in polarity direction at ~350 cm in NWR 5 and at ~274 cm in 96/12-1pc (Fig. 5), suggests that the change from arenaceous to calcareous faunas may have occurred 40–50 kyr earlier in the Arctic’s southwest margin (NWR 5) before transgressing into the central Arctic Ocean (96/12-1pc).

The position of a decrease in magnetic inclination, which has been interpreted as the Brunhes-Matuyama boundary (Poore et al., 1993) or a prominent excursion in the Brunhes Chron (Jakobsson et al., 2000a), occurs consistently between peaks F6 and F7 in core 96/12-1pc, and between the corresponding peaks (K1-K2) in NWR 5 (Fig. 5). This correspondence of independent magneto- and biostratigraphic characteristics lends confidence to the proposed correlation, regardless of whether the inclination record is interpreted as a reversal boundary or an excursion.

A comparison of core 96/12-1pc with CESAR cores from the Alpha Ridge shows a convincing similarity in foraminiferal compositions, based on the > 63 µm size class (Fig. 6; Scott et al., 1989). At both sites, the upper part of the stratigraphic section (F1 to F4 in 96/12-1pc), corresponding to Clark’s unit M on the Alpha Ridge, has high content of *Buliminella elegantissima hensoni* and consistent occurrences of *O. tener/O. umbonatus* (through F3). Below F3, *B. e. hensoni* is replaced by *Bolivina arctica* as the dominant species and *O. tener/O. umbonatus* is virtually absent.

Another correlation based on biostratigraphy was suggested by Jakobsson (2002), by linking fluctuations of nannofossil abundance peaks during MIS 5.5, 5.3 and 5.1 in core 96/12-1pc (Jakobsson et al., 2000a) from the Lomonosov Ridge with concentration fluctuations of dinoflagellate taxa in core PS2138-1 (Knies et al., 1999; Matthiessen et al., 2001) from the Barents Sea margin (Figs. 2 and 5). Matthiessen and colleagues suggest that dinoflagellate cyst events are caused by variable inflow of relatively warm Atlantic water into the Arctic Ocean during periods of warm climate conditions. Calcareous nannofossil peaks in core 96/12-1pc from the Lomonosov Ridge can be clearly correlated to core PS2208-2

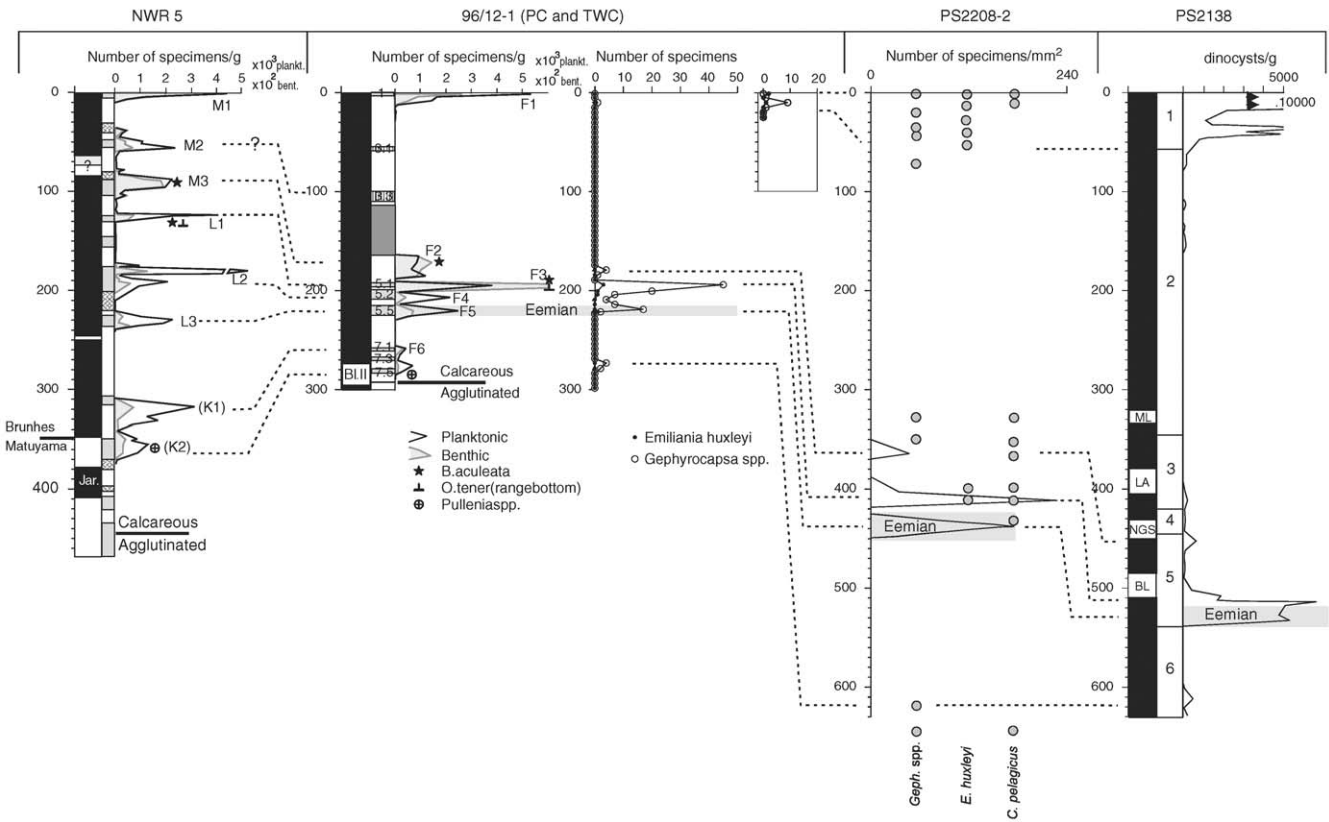


Fig. 5. Correlation of foraminiferal stratigraphies in cores 96/12-1 (Jakobsson et al., 2001; this paper) and NWR 5 (=PI88-P5) (Poore et al., 1993, 1994). Interglacial brown-mud units are shaded; criss-cross pattern in NWR 5 column shows detrital carbonate layers. Curves show numbers of planktic ($\times 10^3$) and benthic ($\times 10^2$, shaded) $> 1.50 \mu\text{m}$ foraminifers per gram sediment. Letters in foraminiferal-peak indices in NWR 5 correspond to Clark's et al. (1980) lithologic units (see also Poore et al., 1994). Indices within unit K (in parentheses) are added. Selected biostratigraphic markers are shown. The position of the Brunhes/Matuyama boundary in NWR 5 reflects the interpretation of Poore et al. (1993, 1994).

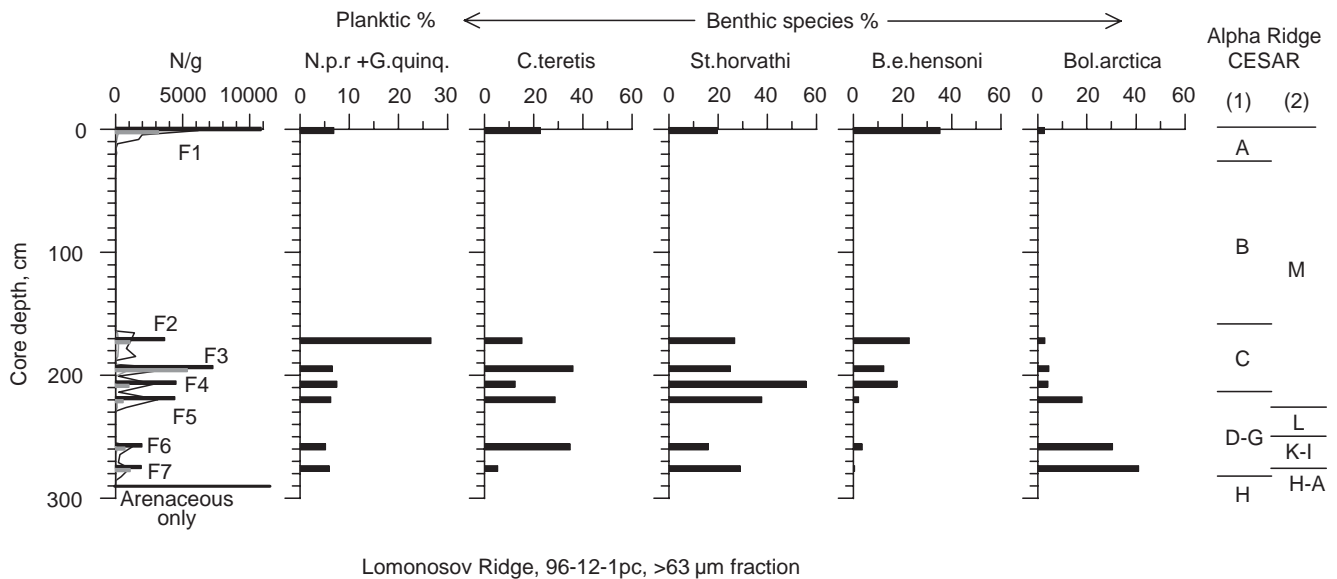


Fig. 6. Major features of the distribution of $> 63 \mu\text{m}$ foraminifers in core 96/12-1pc (bar). Foraminiferal peaks are designated F1 to F7. Curves in the first panel show $> 125 \mu\text{m}$ foraminiferal numbers (N/g = Numbers/g sediment). Column on right side shows correlation with the CESAR cores (Scott et al., 1989): (1) Foraminiferal assemblages, (2) Clark's et al. (1980) lithologic units. N.p.r. = *Neogloboquadrina pachyderma* right-coiled; G. quinq. = *Globigerina* (= *Turborotalita*) *quinqueloba*.

(Gard, 1993, Fig. 5) from the western Nansen Basin (Fig. 5). By using such biostratigraphic signals caused by glacial/interglacial climatic variability, it is possible to correlate cores from the Eurasian margin, via the Nansen Basin to the Lomonosov Ridge, and further to the Amerasia margin, a distance exceeding 2600 km (Figs. 2 and 5).

9. Summary and conclusions

Deciphering the paleoenvironmental history of the Arctic Ocean requires a thorough understanding of age/depth relationships in sediment cores retrieved from its basins and ridges. At present, two contrasting age model scenarios exist, one implying that the central Arctic Ocean has been starved of sediments throughout Plio–Pleistocene times, resulting in mm/ka-scale sedimentation rates, the other implying that the sediment input yielded cm/ka-scale rates over tens of millions of years. The two scenarios thus differ by roughly one order of magnitude.

The litho- and chronostratigraphic model of Clark et al. (1980) is at the centre of the low sedimentation rate scenario, commonly resulting in sub-millimetre rates in cores raised from the Amerasia Basin. This age model is based on paleomagnetic data that by-and-large lack independent age control, and in which the first down-core zone with negative inclination is interpreted to be the Brunhes/Matuyama boundary. At the time when this age model was established, the presence of short time paleomagnetic excursions was not yet well understood, and thus reflects the common practice at that time to assign the first down-core prominent negative inclination to the Brunhes/Matuyama boundary.

We propose a correlation of sedimentary records across the Arctic Ocean that allows us a direct comparison of age models developed for sediment cores from various parts of that ocean. Analysis of the composition of benthic foraminifers permits a correlation of sediment cores from the Lomonosov Ridge to the Alpha Ridge and the Northwind Ridge, that is, across the Amerasia Basin. This correlation is further extended into and through the Eurasia Basin by means of matching nannofossil and dinocyst abundance peaks. In the centre of this correlation transect is a critical Lomonosov Ridge core (96/12-1pc) that has been subjected to rigorous chronostratigraphic analysis using paleomagnetic stratigraphy, nannofossil biostratigraphy, cyclostratigraphy, and OSL dating. These internally consistent data demonstrate that the Brunhes Chron in the Arctic Ocean sediments holds several geomagnetic excursions of short duration. The first down-core zone of negative inclination in this Lomonosov Ridge core is interpreted as the Biwa II excursion at 295 ka. In cores from the Northwind and Alpha Ridges, the correlatable

geomagnetic event has been interpreted as the Brunhes/Matuyama boundary at 780 ka. This comparison clearly answers two of our main initial questions: We do not have two distinctly different modes of deposition that governed the Plio–Pleistocene sedimentation in the Amerasia and Eurasia Basins, but rather two different, non-compatible age models.

Estimates of long-term sedimentation rates derived from total sediment thickness and bedrock ages based on current tectonic models consistently yield cm/ka-scale average ‘pelagic’ sedimentation rates in the central Arctic Ocean, including the Lomonosov Ridge and the Alpha-Mendeleev Ridge complex. This is not surprising, considering the general physiographic setting of the Arctic Ocean, a small basin surrounded by huge landmasses since Cretaceous times, which have yielded km-thick deposits on its abyssal plains.

The Eurasia Basin is connected to the World Ocean via a single narrow, deep conduit, the Fram Strait. It is as yet unclear whether or not the Eurasia and Amerasia Basins are connected through the Lomonosov Ridge at water depths > 1 km. Nevertheless, the relative isolation of the deep Arctic Basins suggests that glacial deep-water ^{14}C reservoir corrections in these basins may have been substantially underestimated, resulting in anomalously young ^{14}C age estimates and low sedimentation rates.

We infer that the seemingly consistent distribution of cores in Fig. 2, in which cm/ka-scale rate cores chiefly occur in the Eurasia Basin and mm/ka-scale rate cores are concentrated in the Amerasia Basin, reflect a bias stemming from inadequate age models giving artificially low sedimentation rates for the Amerasia Basin.

Erosion and/or winnowing may have resulted in reduced net sedimentation rates in various depositional settings (e.g. ridges, abyssal plains) in the central Arctic Ocean. This re-organisation of sediment flow within the Arctic Basin is however fully compatible with our two major conclusions:

The Late Neogene formation of a sea-ice cover in the Arctic Ocean did not markedly inhibit the supply of material to Arctic’s seafloor.

The central Arctic Ocean has not been, on average, a sediment starved basin during either Plio–Pleistocene or pre-Pliocene times, and cm/ka-scale sedimentation rates are the rule rather than the exception throughout this small, land-locked ocean basin.

Acknowledgements

We thank Ruth Jackson for sharing a digital version of her sediment thickness isopach map, and David Mosher and Calvin Campbell for providing samples from the CESAR cores. We thank Ted Moore and John

Hall for valuable discussions and comments. Constructive reviews offered by Jens Matthiessen and an anonymous reviewer contributed to improve the manuscript. Input by Otto Hermelin is also appreciated. We gratefully acknowledge the support by the Swedish Research Council to Jan Backman and by NOAA Grant NA97OG0241 to Martin Jakobsson.

References

- AARI, 1985. Arctic Atlas. Arctic and Antarctic Research Institute, Moscow, Russia (in Russian).
- Aksu, A.E., 1985. Paleomagnetic stratigraphy of CESAR cores. In: Jackson, H.R., Mudie, P.J., Blasco, S.M. (Eds.), Initial Geological Report on CESAR—The Canadian Expedition to study the Alpha Ridge, Arctic Ocean. Geological Survey of Canada Paper, 84–22, pp. 101–114.
- Aksu, A.E., Mudie, P.J., 1985. Magnetostratigraphy and palynology demonstrate at least 4 million years of Arctic sedimentation. *Nature* 318, 280–283.
- Aksu, A.E., Mudie, P.J., Macko, S.A., de Vernal, A., 1988. Upper Cenozoic history of the Labrador Sea, Baffin Bay, and the Arctic Ocean, a paleoclimatic and paleoceanographic summary. *Paleoceanography* 5, 519–538.
- Aldahan, A., Possnert, G., Scherer, R., Shi, N., Backman, J., Boström, K., 2000. Trace-element and major-element stratigraphy in Quaternary sediments from the Arctic Ocean and implications for glacial termination. *Journal of Sedimentary Research* 70, 1095–1106.
- Backman, J., Raffi, I., 1997. Calibration of Miocene nannofossil events to orbitally tuned cyclostratigraphies from Ceara Rise. *Proceedings of the Ocean Drilling Program, Scientific Results* 154, 83–99.
- Baumann, M., 1990. Coccoliths in sediments of the eastern Arctic Basin. In: Bleil, U., Thiede, J., (Eds.), *Geological History of the Polar Oceans: Arctic Versus Antarctic*, NATO ASI Series C, Vol. 108, pp. 437–445. Kluwer, Dordrecht.
- Berggren, W.A., Kent, D.V., Van Couvering, J., 1985. The Neogene: Part 2. Neogene geochronology and chronostratigraphy. In: Snelling, N.J. (Ed.), *The Chronology of the Geological Record*. Geological Society of London Memoir 10, 211–260.
- Berggren, W.A., Kent, D.V., Swisher III, C.C., Aubry, M.-P., 1995. A revised Cenozoic geochronology and chronostratigraphy. *SEPM Special Publication* 54, 129–212.
- Bleil, U., Gard, G., 1989. Chronology and correlation of Quaternary magnetostratigraphy and nannofossil biostratigraphy in Norwegian-Greenland Sea sediments. *Geologische Rundschau* 78, 1173–1187.
- Bukry, D., 1984. Paleogene paleoceanography of the Arctic Ocean is constrained by the middle or late Eocene age of USGS Core FI-422: evidence from silicoflagellates. *Geology* 12, 199–201.
- Cande, S.C., Kent, D.V., 1992. A new geomagnetic polarity time scale for the Late Cretaceous and Cenozoic. *Journal of Geophysical Research* 97, 13917–13951.
- Cande, S.C., Kent, D.V., 1995. Revised calibration of the geomagnetic polarity timescale for the Late Cretaceous and Cenozoic. *Journal of Geophysical Research* 100, 6093–6095.
- Clark, D.L., 1970. Magnetic reversals and sedimentation rates in the Arctic Basin. *Geological Society of America Bulletin* 81, 3129–3134.
- Clark, D.L., 1971. Arctic Ocean ice cover and its Late Cenozoic history. *Geological Society of America Bulletin* 82, 3313–3324.
- Clark, D.L., 1974. Late Mesozoic and Early Cenozoic sediment cores from the Arctic Ocean. *Geology* 2, 41–44.
- Clark, D.L., 1990. Arctic Ocean ice cover; Geologic history and climatic significance. In: Grantz, A. et al. (Eds.), *The Arctic Ocean Region*, Vol. L. Geological Society of America, *The Geology of North America*, Boulder, pp. 53–62.
- Clark, D.L., 1996. The Pliocene record in the central Arctic Ocean. *Marine Micropaleontology* 27, 157–164.
- Clark, D.L., Hanson, A., 1983. Central Arctic Ocean sediment texture: a key to ice transport mechanisms. In: Molnia, B.F. (Ed.), *Glacial-Marine Sedimentation*. Plenum Press, New York, pp. 301–330.
- Clark, D.L., Whitman, R.R., Morgan, K.A., Mackay, S.D., 1980. Stratigraphy and glacial-marine sediments of the Basin, central Arctic Ocean. *Geological Society of America Special Paper* 181, 1–57.
- Clark, D.L., Vincent, J.-S., Jones, G.A., Morris, W.A., 1984. Correlation of marine and continental glacial and interglacial events, Arctic Ocean and Banks Island. *Nature* 311, 147–149.
- Clark, D.L., Kowallis, B.J., Medaris, L.G., Deino, A.L., 2000. Orphan Arctic Ocean metasediment clast: local derivation from alpha ridge pre-2.6 Ma ice rafting? *Geology* 28, 1143–1146.
- Coe, R.S., Liddicoat, J.C., 1994. Overprinting of a natural magnetic remanence in lake sediments by a subsequent high-intensity field. *Nature* 367, 57–59.
- Darby, D.A., Naidu, A.S., Mowatt, T.C., Jones, G., 1989. Sediment composition and sedimentary processes in the Arctic Ocean. In: Herman, Y. (Ed.), *The Arctic Seas*. Van Nostrand Reinhold Company, New York, pp. 657–720.
- Darby, D.A., Bischof, J.F., Jones, G.A., 1997. Radiocarbon dating of depositional regimes in the western Arctic Ocean. *Deep-Sea Research II* 44, 1745–1757.
- Doyle, P.S., Riedel, W.R., 1979. Cretaceous to Neogene ichtyoliths in a giant piston core from the central North Pacific. *Micropaleontology* 25, 337–364.
- Eicken, H., Kolatschek, J., Freitag, J., Lindemann, F., Kassens, H., 2000. A key source area and constraints on entrainment for basin-scale sediment transport by Arctic Ocean. *Geophysical Research Letters* 27, 1919–1922.
- Elverhøi, A., Hooke, R.L.B., Solheim, A., 1998. Late Cenozoic erosion and sediment yield from the Svalbard–Barents Sea Region: implications for understanding erosion of glacierized basins. *Quaternary Science Reviews* 17, 209–241.
- Frederichs, T., 1995. Regional and temporal variations of rock magnetic parameters in Arctic marine sediments. *Berichte zur Polarforschung* 164, 1–212.
- Gard, G., 1993. Late Quaternary coccoliths at the North Pole: evidence of ice-free conditions and rapid sedimentation in the central Arctic Ocean. *Geology* 21, 227–230.
- Grantz, A., May, S.D., Taylor, P.T., Lawver, L.A., 1990. Canada Basin. In: Grantz, A. et al. (Eds.), *The Arctic Ocean Region*, Vol. L. Geological Society of America, *The Geology of North America*, Boulder, pp. 379–402.
- Grantz, A., Phillips, R.L., Mullen, M.W., Starratt, S.W., Jones, G.A., Sathy Naidu, A., Finney, B.P., 1996. Character, paleoenvironment, rate of accumulation, and evidence for seismic triggering of Holocene turbidites, Canada Abyssal Plain, Arctic Ocean. *Marine Geology* 133, 51–73.
- Grantz, A., Phillips, R.L., Jones, G.A., 1999. Holocene pelagic and turbidite sedimentation rates in the Amerasia Basin, Arctic Ocean from radiocarbon age-depth profiles in cores. *GeoResearch Forum* 5, 209–222.
- Grantz, A., Pease, V.L., Willard, D.A., Phillips, R.L., Clark, D.L., 2001. Bedrock cores from 89° North: implications for the geologic framework and Neogene paleoceanography of Lomonosov Ridge and a tie to the Barents shelf. *Geological Society of America Bulletin* 113, 1272–1281.

- Gubbins, D., 1999. The distinction between geomagnetic excursions and reversals. *Geophysical Journal International* 137, F1–F3.
- Hall, J.K., 1979. Sediment waves and other evidence of paleo-bottom currents at two locations in the deep Arctic Ocean. *Marine Geology* 23, 269–299.
- Herman, Y., 1974. Arctic Ocean sediments, microfauna, and the climatic record in late Cenozoic time. In: Herman, Y. (Ed.), *Marine Geology and Oceanography of the Arctic Seas*. Springer, Berlin, pp. 283–348.
- Hilgen, F.J., 1991. Extension of the astronomically calibrated (polarity) time scale to the Miocene/Pliocene boundary. *Earth Planetary Science Letters* 107, 349–368.
- Hunkins, K., Bé, A.W.H., Opdyke, N.D., Mathieu, G., 1971. The Late Cenozoic history of the Arctic Ocean. In: Turekian, K.K. (Ed.), *The Late Cenozoic Glacial Ages*. Yale University Press, New Haven, pp. 215–237.
- Ishman, S.E., Polyak, L.V., Poore, R.Z., 1996. Expanded record of Quaternary oceanographic change: Amerasian Arctic Ocean. *Geology* 24, 139–142.
- Jakobsson, M., 2002. Hypsometry and volume of the Arctic Ocean and its constituent seas. *Geochemistry, Geophysics, Geosystems* 3, 1–18.
- Jakobsson, M., Løvlie, R., Al-Hanbali, H., Arnold, E., Backman, J., Mörth, M., 2000a. Manganese and color cycles in Arctic Ocean sediments constrain Pleistocene chronology. *Geology* 28, 23–26.
- Jakobsson, M., Cherkis, N., Woodward, J., Coakley, B., Macnab, R., 2000b. A new grid of arctic bathymetry: a significant resource for scientists and mapmakers. *EOS Transactions, American Geophysical Union* 81 (89), 93–96.
- Jakobsson, M., Løvlie, R., Arnold, E.M., Backman, J., Polyak, L., Knutsen, J.-O., Musatov, E., 2001. Pleistocene stratigraphy and paleoenvironmental variation from Lomonosov Ridge sediments, central Arctic Ocean. *Global and Planetary Change* 31, 1–22.
- Jakobsson, M., Grantz, A., Kristoffersen, Y., Macnab, R., 2003a. Physiographic provinces of the Arctic Ocean. *Geological Society of America Bulletin* 115, December 2003.
- Jakobsson, M., Backman, J., Murray, A., Løvlie, R., 2003b. Optically stimulated luminescence dating supports central Arctic Ocean cm-scale sedimentation rates. *Geochemistry, Geophysics, Geosystems* 4, 1–11.
- Jackson, H.R., Oakey, G.N., 1990. Sedimentary thickness map of the Arctic Ocean. In: Grantz, A. et al. (Eds.), *The Arctic Ocean Region, Vol. L. Geological Society of America, The Geology of North America, Boulder, Plate 5*.
- Jackson, H.R., Forsyth, D.A., Hall, J.K., Overton, A., 1990. Seismic reflection and refraction. In: Grantz, A. et al. (Eds.), *The Arctic Ocean Region, Vol. L. Geological Society of America, The Geology of North America, Boulder*, pp. 153–170.
- Jacobs, J.A., 1994. *Reversals of the Earth's Magnetic Field*. Cambridge University Press, Cambridge, pp. 1–346.
- Johnson, G.L., 1969. Morphology of the Eurasian Arctic Basin. *Polar Record* 14, 619–628.
- Jokat, W., 2003. Seismic investigations along the western sector of Alpha Ridge, Central Arctic Ocean. *Geophysical Journal International* 152, 185–201.
- Jokat, W., Uenzelmann-Neben, G., Kristoffersen, Y., Rasmussen, T., 1992. ARCTIC'91: Lomonosov Ridge—a double sided continental margin. *Geology* 20, 887–890.
- Jokat, W., Weigelt, E., Kristoffersen, Y., Rasmussen, T., Schöne, T., 1995. New insights into the evolution of the Lomonosov Ridge and the Eurasian Basin. *Geophysical Journal International* 122, 378–392.
- Jokat, W., Stein, R., Rachor, E., Schewe, I., Shipboard Scientific Party, 1999a. Expedition gives fresh view of Central Arctic geology. *EOS Transactions American Geophysical Union* 80(465), 472–473.
- Jokat, W. (Ed.), and shipboard participants, 1999b. ARCTIC '98: The Expedition ARK-XIV/1a of RV "Polarstern" in 1998. *Berichte zur Polarforschung* 308, 1–159.
- Jones, G.A., 1987. The central Arctic Ocean sediment record: current progress in moving from a litho- to a chronostratigraphy. *Polar Research* 5, 309–311.
- Kennett, J.P., Srinivasan, M.S., 1983. *Neogene Planktonic Foraminifera*. Hutchinson Ross Publishing Company, Stroudsburg, PA, pp. 1–165.
- Knies, J., Vogt, C., Stein, R., 1999. Late Quaternary growth and decay of the Svalbard/Barents Sea ice sheet and paleoceanographic evolution in the adjacent Arctic Ocean. *Geo-Marine Letters* 18, 195–202.
- Kristoffersen, Y., 1990. Eurasia Basin. In: Grantz, A. et al. (Eds.), *The Arctic Ocean Region, Vol. L. Geological Society of America, The Geology of North America, Boulder*, pp. 365–378.
- Kristoffersen, Y., Husebye, E.S., 1985. Multi-channel seismic reflection measurements in the Eurasia Basin, Arctic Ocean, from the US ice station FRAM IV. *Tectonophysics* 114, 103–115.
- Kucera, M., Kennett, J.P., 2002. Causes and consequences of a middle Pleistocene origin of the modern planktonic foraminifer *Neogloboquadrina pachyderma* sinistral. *Geology* 30, 539–542.
- LaBrecque, J.L., Kent, D.V., Cande, S.C., 1977. Revised magnetic polarity time scale for late cretaceous and cenozoic time. *Geology* 5, 330–335.
- Langereis, C.G., Dekkers, M. J., de Lange, G.J., Paterne, M., van Santvoort, P.J.M., 1997. Magnetostratigraphy and astronomical calibration of the last 1.1 Ma from an eastern Mediterranean piston core and dating of short events in the Brunhes. *Geophysical Journal International* 129, 75–94.
- Lawver, L.A., Scotese, C.R., 1990. A review of tectonic models for the evolution of the Canada Basin. In: Grantz, A. et al. (Eds.), *The Arctic Ocean Region, Vol. L. Geological Society of America, The Geology of North America, Boulder, Vol. L*, pp. 593–618.
- Lindemann, F., Hölemann, J.A., Korablev, A., Zachek, A., 1999. Particle entrainment into newly forming sea ice—freeze-up studies in October 1995. In: Kassens, H., et al. (Ed.), *Land-Ocean Systems in the Siberian Arctic: Dynamics and History*. Springer, Berlin, pp. 113–123.
- Løvlie, R., 1994. Field-dependent postdepositional grain realignment in the PDRM process: experimental evidence and implications. *Physics of the Earth and Planetary Interiors* 85, 101–111.
- Løvlie, R., Markussen, B., Sejrup, H.-P., Thiede, J., 1986. Magnetostratigraphy in three Arctic Ocean cores; arguments for geomagnetic excursions within oxygen-isotope stage 2–3. *Physics of the Earth and Planetary Interiors* 43, 173–184.
- Macko, S.A., Aksu, A.E., 1986. Amino acid epimerization in planktonic foraminifera suggests slow sedimentation rates for Alpha Ridge, Arctic Ocean. *Nature* 322, 730–732.
- Markussen, B., Zahn, R., Thiede, J., 1985. Late Quaternary sedimentation in the eastern Arctic Basin: stratigraphy and depositional environment. *Palaeogeography, Palaeoclimatology, Palaeoecology* 50, 271–284.
- Matthiessen, J., Knies, J., Nowaczyk, N.R., Stein, R., 2001. Late Quaternary dinoflagellate cyst stratigraphy at the Eurasian continental margin, Arctic Ocean: indications for Atlantic water inflow in the past 150,000 years. *Global and Planetary Change* 31, 65–86.
- Menard, H.W., Smith, S.M., 1966. Hypsometry of Ocean Basin provinces. *Journal of Geophysical Research* 71, 4305–4325.
- Minicucci, D.A., Clark, D.L., 1983. A Late Cenozoic stratigraphy for glacial-marine sediments of the eastern Alpha Cordillera, central Arctic Ocean. In: Molnia, B.F. (Ed.), *Glacial-marine sedimentation*. Plenum Press, New York, pp. 331–365.

- Morris, T.H., Clark, D.L., Blasco, S.M., 1985. Sediments of the Lomonosov Ridge and Makarov Basin: a Pleistocene stratigraphy for the North Pole. *Geological Society of America Bulletin* 96, 901–910.
- Nørgaard-Pedersen, N., Spielhagen, R.F., Thiede, J., Kassens, H., 1998. Central Arctic surface ocean environment during the past 80,000 years. *Paleoceanography* 13, 193–204.
- Nowaczyk, N.R., Baumann, M., 1992. Combined high-resolution magnetostratigraphy and nannofossil biostratigraphy for Late Quaternary Arctic Ocean sediments. *Deep-Sea Research* 39, 567–601.
- Nowaczyk, N.R., Knies, J., 2000. Magnetostratigraphic results from the eastern Arctic Ocean: AMS ^{14}C ages and relative palaeointensity data of the Mono Lake and Laschamp geomagnetic reversal excursions. *Geophysical Journal International* 140, 185–197.
- Nowaczyk, N.R., Frederichs, T.W., Eisenhauer, A., Gard, G., 1994. Magnetostratigraphic data from Late Quaternary sediments from the Yermak Plateau, Arctic Ocean. Evidence for four geomagnetic polarity events within the last 170 Ka of the Brunhes Chron. *Geophysical Journal International* 117, 453–471.
- Nowaczyk, N.R., Frederichs, T.W., Kassens, H., Nørgaard-Pedersen, N., Spielhagen, R., Stein, R., Weiel, D., 2001. Sedimentation rates in the Makarov Basin, central Arctic Ocean: a paleomagnetic and rock magnetic approach. *Paleoceanography* 16, 368–389.
- Nürnberg, D., Wollenburg, I., Dethleff, D., Eicken, H., Kassens, H., Letzig, T., Reimnitz, E., Thiede, J., 1994. Sediments in Arctic sea ice: implications for entrainment transport and release. *Marine Geology* 119, 184–214.
- Payne, M.A., Verosub, K.L., 1982. The acquisition of post-depositional detrital remanent magnetization in a variety of natural sediments. *Geophysical Journal of Royal Astronomical Society* 68, 625–642.
- Peterson, B.J., Holmes, R.M., McClelland, J.W., Vörösmarty, C.J., Lammers, R.B., Shiklomanov, A.I., Shiklomanov, I.A., Rhamstorf, S., 2002. Increasing river discharge to the Arctic Ocean. *Science* 298, 2171–2173.
- Pfirman, S., Lange, M.A., Wollenburg, I., Schlosser, P., 1990. Sea ice characteristics and the role of sediment inclusions in deep-sea deposition: Arctic-Antarctic comparisons. In: Bleil, U., Thiede, J. (Eds.), *Geological History of the Polar Oceans: Arctic Versus Antarctic*. NATO ASI Series C, Vol. 108, pp. 187–211.
- Phillips, L.R., Grantz, A., 1997. Quaternary history of sea ice and paleoclimate in the Amerasia Basin, Arctic Ocean, as recorded in the cyclical strata of Northwind Ridge. *Geological Society of America Bulletin* 109, 1101–1115.
- Phillips, R.L., Grantz, A., 2001. Regional variations in provenance and abundance of ice-rafted clasts in Arctic Ocean sediments: implications for the configuration of Late Quaternary oceanic and atmospheric circulation in the arctic. *Marine Geology* 172, 91–115.
- Polyak, L.V., 1986. New data on microfauna and stratigraphy of bottom sediments of the Mendeleev Ridge, Arctic Ocean. In: Andreev, S.I. (Ed.), *Sedimentogenesis and Nodule-Formation in the Ocean*. Sevmorgeologia, Leningrad, pp. 40–50 (in Russian).
- Poore, R.Z., Phillips, R.L., Rieck, H.J., 1993. Palaeoclimate record for Northwind Ridge, Western Arctic Ocean. *Paleoceanography* 8, 149–159.
- Poore, R.Z., Ishman, S.E., Phillips, L., McNeil, D., 1994. Quaternary stratigraphy and paleoceanography of the Canada Basin, western Arctic Ocean. *US Geological Survey Bulletin* 2080, 1–32.
- Schneider, D.A., Backman, J., Curry, W.B., Possnert, G., 1996. Paleomagnetic constraints on sedimentation rates in eastern Arctic Ocean. *Quaternary Research* 46, 62–71.
- Scott, D.B., Mudie, P.J., Baki, V., MacKinnon, K.D., Cole, F.E., 1989. Biostratigraphy and Late Cenozoic paleoceanography of the Arctic Ocean: foraminiferal, lithostratigraphic, and isotopic evidence. *Geological Society of America Bulletin* 101, 260–277.
- Sejrup, H.P., Gifford, H.M., Brigham-Grette, J., Løvlie, R., Hopkins, D., 1984. Amino acid epimerization implies rapid sedimentation rates in Arctic ocean cores. *Nature* 310, 772–775.
- Shackleton, N.J., Berger, A., Peltier, W.R., 1990. An alternative astronomical calibration of the lower Pleistocene timescale based on ODP Site 677. *Transactions of the Royal Society of Edinburgh* 81, 251–261.
- Shackleton, N.J., Crowhurst, S., Hageberg, T., Pisias, N.G., Schneider, D.A., 1995. A new late Neogene time scale: application to leg 138 sites. *Proceedings of the Ocean Drilling Program, Scientific Results* 138, 73–101.
- Shackleton, N.J., Crowhurst, S.J., Weedon, G.P., Laskar, J., 1999. Astronomical calibration of Oligocene-Miocene time. *Philosophical Transactions of the Royal Society* 357, 1907–1929.
- Sikes, E.L., Samson, C.R., Guilderson, T.P., Howard, W.R., 2000. Old radiocarbon ages in the southwest Pacific Ocean during the last glacial period and deglaciation. *Nature* 405, 555–559.
- Smith, J. D., Foster, J.H., 1969. Geomagnetic reversal in Brunhes normal polarity epoch. *Science* 163, 565–567.
- Spielhagen, R.F., Bonani, G., Eisenhauer, A., Frank, M., Frederichs, T., Kassens, H., Kubik, P.W., Mangini, A., Nørgaard-Pedersen, N., Nowaczyk, N.R., Schäper, S., Stein, R., Thiede, J., Tiedemann, R., Wachsner, M., 1997. Arctic Ocean evidence for Late Quaternary initiation of northern Eurasian ice sheets. *Geology* 25, 783–786.
- Stein, R., Schubert, C., Vogt, C., Fütterer, D., 1994. Stable isotope stratigraphy, sedimentation rates, and salinity changes in the latest Pleistocene to Holocene eastern central Arctic Ocean. *Marine Geology* 119, 333–355.
- Stein, R., Steinke, T., Dittmers, K., Fahl, K., Kraus, M., Matthiessen, J., Niessen, F., Pirrung, M., Polyakova, Ye., Schoster, F., Fütterer, D.K., 2004. Arctic (paleo) river discharge and environmental change: evidence from the Holocene Kara Sea sedimentary records. *Quaternary Science Reviews*, this issue (doi:10.1016/j.quasci-rev.2003.12.004).
- Steuerwald, B.A., Clark, D.L., Andrew, J.A., 1968. Magnetic stratigraphy and faunal patterns in Arctic Ocean sediments. *Earth and Planetary Science Letters* 5, 79–85.
- Svindland, K.T., Vorren, T.O., 2002. Late Cenozoic sedimentary environments in the Amundsen Basin, Arctic Ocean. *Marine Geology* 186, 541–555.
- Sweeney, J.F., 1985. Comments about the age of the Canada Basin. *Tectonophysics* 114, 1–10.
- Tiedemann, R., Sarnthein, M., Shackleton, N.J., 1994. Astronomic timescale for the Pliocene Atlantic $\delta^{18}\text{O}$ and dust flux records of Ocean Drilling Program Site 659. *Paleoceanography* 9, 619–638.
- Thierstein, H.R., Geitzenauer, K.R., Molfino, B., Shackleton, N.J., 1977. Global synchronicity of Late Quaternary coccolith datum levels: validation by oxygen isotopes. *Geology* 5, 400–404.
- van Donk, J., Mathieu, G., 1969. Oxygen isotope compositions of foraminifera and water samples from the Arctic Ocean. *Journal of Geophysical Research* 74, 3369–3407.
- Verosub, K.L., 1975. Paleomagnetic excursions as magnetostratigraphic horizons: a cautionary note. *Science* 190, 48–50.
- Verosub, K.L., 1982. Geomagnetic excursions: a critical assessment of the evidence as recorder in sediments of the Brunhes Epoch. *Philosophical Transactions Royal Society London A* 306, 161–168.
- Watkins, N.D., 1968. Short period geomagnetic polarity events in deep-sea sedimentary cores. *Earth and Planetary Science Letters* 4, 341–349.

- Weber, J.R., Roots, E.F., 1990. Historical background; Exploration, concepts, and observations. In: Grantz, A., et al. (Eds.), *The Arctic Ocean Region*, Vol. L. Geological Society of America, The Geology of North America, Boulder, pp. 5–36.
- Weber, J.R., Sweeney, J.F., 1990. Ridges and basins in the central Arctic Ocean. In: Grantz, A., et al. (Eds.), *The Arctic Ocean Region*, Vol. L. Boulder, Geological Society of America, The Geology of North America, Boulder, pp. 305–336.
- Witte, W.K., Kent, D.V., 1988. Revised magnetostratigraphies confirm low sedimentation rates in Arctic Ocean cores. *Quaternary Research* 29, 43–53.